Thesis for the Degree of Master of Science

HABITABLE ENVIRONMENTS OF EXTRASOLAR PLANET'S MOON

Byeong-Chol Lee

Department of Astronomy and Atmospheric Sciences
The Graduate School

December 2000

The Graduate School
Kyungpook National University

Habitable Environments of Extrasolar Planet's moon

Byeong-Chol Lee

Department of Astronomy and Atmospheric Sciences
The Graduate School

Supervised by Professor Myeong-Gu Park

Approved as a qualified thesis of Byeong-Chol Lee
for the degree of Master of Science
by the Evaluation Committee

December 2000

Chairman _____

_____

_____

The Graduate School Council, Kyungpook National University

Contents

List of Tables

List of Figures

Chapter 1

INTRODUCTION

For several decades, the search for extra terrestrial intelligence (SETI) has been an important issue of astronomy as well as of biology, geology, and religion. The search for extra-solar planets, which is considered, in a broad sense, to be able to supply indirect evidence of SETI, have practically started since mid 1990's. Mayor & Queloz (1995) first detected a 'planet-like companion' to a main sequence star 51 Peg. Since then, the true nature of extra-solar planet (hereafter, exoplanet) has become publicly acknowledged.

Most current searching programs are based on high precision radial velocity measurement and long term detailed monitoring of late F and G type stars, e.g., ELODIE survey (Soubiran, Katz, & Cayrel 1998; Katz et al. 1998; Baranne et al. 1996), CORALIE survey (Santos et al. 2000a, 2000b; Udry et al. 2000; Queloz et al. 2000a, 2000b). A total of 46 confirmed exoplanetary systems are discovered by this method as

of November 2000, and the number is growing steadily. Photometric methods have been briefly considered over the last few years (Schneider 2000; Jenkins et al. 2000; Jha et al. 2000; Gaudi 2000; Brown 2000; Henry et al. 2000; Fortney et al. 2000; Dunham 1999; Borucki et al. 1998; Esquerdo 1988; Guinan et al. 1997; Deeg et al. 1997), but are generally thought to be unable to reach the necessary precision levels without resorting to expensive space missions.

As the region of supporting a life, so called 'habitable zone' (HZ) (Huang 1959; Shklovski & Sagan 1966; Hart 1979), exoplanets arouse astronomer' interest in life. Recently, Kasting, Whitmire, & Reynolds (1993) estimate the width of the HZ around our Sun and other main sequence stars. They only consider Earth-like planets with atmospheres composed of CO_2, H_2O and N_2 (except O_2), which is required for the existence of liquid water on the surface of a planet.

At present, the masses of known exoplanets are limited to be near or heavier than that of Jupiter (M_J) due to observational difficulties. Moreover, because we do not know the inclination of the orbit (i), which is 0 for face-on, we can only estimate the minimum mass ($M \sin i$). If an exoplanet is composed of heavy elements only, it could collapse gravitationally by degeneration of an exoplanet. Hence, it is thought that all giant exoplanets (hearafter, giantplanets) are composed of gases.

Although the concept of ground based organisms are too restricted the case of life on the Earth suggests that it can be a general criterion.

Hence, Jovian planets or brown dwarfs support neither a solid nor a liquid surface near which organisms might dwell.

Williams, Kasting, & Wade (1997) argued rocky moons around giant-planet which can host ground based life and support liquid water. Because most planets in our solar system have one or more moons, moons around giantplanet would be reasonable possibility.

In this thesis, we assume an Earth-like moon around giantplanet, and investigate the environments of habitability on the moon. In case of a giantplanet more massive than 13 M_J, energy can be given off by deuterium burning. Habitability of a moon around such giantplanet will be affected by the larger amount of energy than the usual stellar energy. So, hear we study giantplanets less than 13 M_J, which is the minimum mass for deuterium burning and brown dwarf threshold.

This thesis consists as follows. In Chapter 2, we summarize known extra-solar planetary systems and explain the searching methods of exoplanets. We consider conditions for the 'habitable zone' in Chapter 3. In Chapter 4, we explain the requirement of a moon around giantplanet and preconditions of stability. We also analyse the environments of extra-solar planet's moon (hereafter, exo-moon) for habitability. In Chapter 5, we show that the habitability in an exo-moon could be changed by stellar luminosity evolution. Then, we, among the known exoplanets, estimate a possible epoch and duration for the emergence of life. We discuss the results in Chapter 6.

Chapter 2

METHODS OF SEARCHING EXOPLANETS AND CANDIDATE STARS

2.1 Planetary Formation and Atmospheric Evolution

Lissauer (1999) predicts that rocky planets would form around most single stars, although it is possible that in some cases such planets may be lost by orbital decay within the protoplanetary disk phase. Terrestrial planets are believed to grow via pair-wise accretion until the spacing of planetary orbits becomes large enough that the configuration is stable for the age of the system. Giantplanets begin their growth like terrestrial planets, but if they become massive enough before the protoplanetary disk dissipates, then they are able to accumulate substantial amounts of

gas. In the sequel stage, they progress like planets in the current Solar planetary system. But, after formed, the timescale for the subsequent evolution of its surface is difficult to be determined precisely.

During the formation of the Earth around primitive solar nebula, light volatile matters are pushed away by solar wind while heavy elements remain. Sequently, after thermal processing of impact and conjunction by primitive planetesimal, atmosphere is formed. Therefore, current planetary atmosphere implies that it is not composed of primitive elements but is formed by the eruption by interior elements. And, because of volcanic eruptions by repeated meteoritic collisions and thermal equilibrium process in the interior, the atmosphere may have become composed of water vapor, CO_2, N_2 gases from the interior.

We can infer the different formation histories of giantplanets and terrestrial planets from the chemical composition of the solar system. According to the standard model for planet formation, giantplanet must be detected beyond 1 AU. Temperature of proto-solar nebular increases as the distance from central star is smaller. Closer to the star, high stellar flux disturbs accumulation of grains (Barshay & Lewis 1976). In greater distances, ice material can be formed due to very low protostellar nebula temperature (Boss 1995, 1996b). This explains not only the chemical composition of terrestrial planets and ice-rich satellites but also the lack of planet inside the Mercury orbit.

2.2 Extrasolar Planetary System

The question of where and how planets form around other stars are one of the most important issues of current astronomy. The *IRAS* data of wavelengths $10 \sim 100$ μm show IR excesses, which are interpreted as evidence of an orbiting disk composed of grains whose sizes are 1 to 100 μm. The generic lifetime of grains is less than the age of the star, and the observed grains must have supplying sources, such as planetesimals (Whitmire, Matese, & Tomley 1988; Backman & Paresce 1992). Extensive modeling of the *IRAS* data and of observations at different wavelengths indicates that the prototype systems (α Lyr, α Psa, β Pic) have gaps or holes in their inner disks with radius in the range of $20 \sim 80$ AU. One possible explanation for the maintenance of these gaps against Poynting-Robertson drag and collisional diffusion is the presence of a planetary system.

At present, stellar mass function indicates that there are approximately 45 million stars (0.0001% of Galaxy) within 1 kpc of the Sun, which is within the current limit of ground based telescope. However, far fewer planetary systems are expected not only because the terrestrial planetary formation process itself may require $10^7 \sim 10^8$ yr to reach completion (Wetherill 1996), but also because stars of spectral type earlier than A5 ($\sim 10^6$ stars) have short lifetimes.

Since Mayor & Queloz (1995) first detected 'planet-like companion'

to the main sequence star 51 Peg, more than forty exoplanets have been found for the past five years. Strictly speaking, Wolszczan, Cordes, & Dewey (1991) already unambiguously identified planets around the pulsar PSR 1257+12. But, this pulsar does not show characteristics of typical planets, and is not an object of bioastronomy.

Several of known exoplanets that are closely encountered with mother star are known as '51 Peg-type star'. In differently standard planetary formation, most detected exoplanets locate close in mother star within approximately 0.05 AU, with large eccentricities and massive giantplanets. In this case, there is unexpected to the standard thesis of star and planetary formation. Four specific mechanisms have been suggested as possible processes to bring a giantplanet into a short-period orbit around star(see Ford, Rasio, & Sills 1999). The first mechanism is a secular interaction with a distant binary companion. The second is dissipation of the protostellar nebular. A resonant interaction with a disk of planetesimals is another possible source of orbital migration. The fourth mechanism is based on dynamical instability of a system originally containing multiple giantplanets of comparable masses.

2.3 Detection Methods

2.3.1 Radial Velocities

When a planet is in orbit around a star, the star wobbles by gravitational perturbation of the planet. So, from variations of radial velocity by spectroscopic measurement, some physical properties of planet can be determined, for example, semi-major axis, revolution period, eccentricity, and the mass of planet. From ground-based observatories, spectroscopists currently can measure Doppler shifts greater than 3 $\mathrm{m\,s^{-1}}$, which corresponds to a minimum detectable mass of 33 $M_\oplus$ for a planet at 1AU from 1 $M_\odot$. Nearly every known exoplanet is detected by this radial velocity measurement.

2.3.2 Astrometry

The angular wobble of a star in response to its companion's orbital motion is proportional to both the mass of planet and the orbital radius, and inversely proportional to the distance to the star. A Jovian mass orbiting 5 AU from a solar-type star that is located 10 pc away would produce an astrometric amplitude of 0.5 milliarcsec. With a space-based astrometric instrument, such as the planned Space Interferometry Mission (SIM), that can measure an angle as small as 2 microarcsec, a minimum planetary mass 6.6 $M_\oplus$ is detectable in one year orbit around a 1 $M_\odot$ star that is 10 pc from the Earth. The ground-based Keck telescope

is being equipped to measure angles as small as 20 microarcsec, leading to a minimum detectable mass in one AU orbit of 66 $M_\oplus$ for 1 $M_\odot$ star at 10 pc.

The planet around Lalande 21185 was detected by optical astrometry, although astrometric curve was not published. Gatewood (1996) has shown astrometric residuals indicating about 30 years drift with 7 σ significance (M=1.6 M_J) and a 2 σ wobble with about 6 years period (M=0.9 M_J).

This method could provide a secure mass of exoplant, contrary to the other detective methods, and offer orbital inclination of a planet.

2.3.3 Transits

Photometry measures the periodic dimming of the star caused by a planet passing in front of the star along the line of sight to the observer. Magnitude drops during this transit allow us to detect planets. Charbonneau et al. (2000) confirmed the transit of exoplanet around HD 209459 using the 0.80 m automatic photoelectric telescope (APT) at Fairborn Observatory in southern Arizona. The estimated duration was 3.1 hours, which was predicted from the stellar radius, the orbital radius and the orbital period determined by the spectroscopic discovery observation. The star showed 0.017 mag brightness drop, which corresponds to a drop in light intensity of $1.58 \pm 0.18\%$. The orbital inclination angle of the planet around HD 209458 is $\sin i > 0.993$, leading to a true mass

of 0.62 M_J for the planet.

2.3.4 Microlensing

Gravitational microlensing in the Galactic bulge may also reveal the presence of planets in orbit around the intervening lensing objects. So, this method can be used to detect light curve of single planet. Bennett et al. (1999) inferred that the lens system consists of a planet of about 3 M_J orbiting a binary at a distance of $\sim$ 1.8 AU. However, the caustic for exoplanet and exo-moon is very weak and only a single event is observed. Nevertheless, microlensing is presently a unique technique in its ability to detect Earth-sized mass planet in orbit with semi-major axis of several AU around a main sequence star from the ground-based telescope.

2.3.5 Direct Imaging and Albedo

We can detect a planet by observing the reflected stellar light from it. When we observe Pluto with high-efficiency telescope, it shines the same as a bright star. In case of far-off stars, however, the detection may be impossible. Even though a planet orbits a star closely, a stellar image always makes a diffraction halo, and we must use a telescope that can remove the diffraction to separate light from the planet. Neuhäuser et al. (2000) show that the detection of exoplanet by ground-based direct imaging is possible with current technology. They present evidence for a possible planetary companion to the young T Tauri star 1RXSJ10423.3-

334014 (TWA-7), detected by ROSAT as a member of the nearby TW Hya association. In an HST NICMOS F160W image, an object is detected that is more than 9 mag fainter than TWA-7. However, TWA-7b could be either a background object or a companion to star, due to large astrometric errors in position angles and separations.

2.4 Candidate Stars

A 'planet' is an object that has a mass between that of Pluto and the deuterium burning threshold, and that forms in orbit around a star that generates energy by nuclear reactions. Objects less massive than 13 M_J never burn deuterium nor generate significant energy from any nuclear reactions. We show currently known exoplanets with respect to orbital semi-major axes in Figure 2.1. The mass distribution shows a clear paucity above 5 M_J. And, the number of systems rises steeply toward smaller masses down to the detection limit near 1 M_J.

We don't see objects more massive than 13 M_J, except the confirmed exoplanets around pulsars and disks (potentially protoplanetary or associated to planets) and unconfirmed (doubtful, unpublished or invalidated) objects. Indicated M_J denote Jovian mass, which corresponds to 318 $M_\oplus$, and each mass denoted is the lower limit of exoplanet. Upsilon And., near the top of the chart, has three companions, and HD 83443, HD 168443 have two companions each. Analysis of the residual

curve in observed data show that the systems must consists of another objects. In addition, data of several exoplanets show irregularities, which may provide chances to find multiple exoplanets under continuous and a well-equipped observation.

Most exoplanets are detected within 2 AU from mother stars, especially about a half of those are found within Mercury orbit, i.e., ~ 0.387 AU. Short orbital period is an advantage in detecting companion mass: A period curve can be constructed without difficulty because an orbital period is only several days. On the other hand, long orbital period systems typically have a period measured in years. For example, the orbital period in ϵ Eri. is about 6.7 years, with plausible error in data.

2.5 Future Observation

Erskine & Ge (1999) develop a prototype fringing spectrograph optimized for sensitive stellar radial velocity measurement, aimed at detecting small velocity perturbation by an exoplanet and stellar seismology on an amplitude of ~ 1 $\mathrm{m\,s^{-1}}$ or less. It is a combination of an angle-independent interferometer and a high throughput intermediate resolution spectrograph. In a test with the Sun, the diurnal velocity variation caused by the Earth's orbit is observed. The Galactic Exoplanet Survey Telescope (Rhie et al. 2000, GEST) will monitor the Galactic bulge for 8 months per three years to detect planets via gravitational microlensing

and transits, which is sensitive to planets with masses as low as that of Mars. This mission is expected to detect about 50,000 planets via transits.

The European Southern Observatory (ESO) is planning to install the VLT Imager and Spectrometer for the InfraRed (VISIR) at the Cassegrain focus of the Melipal, the third unit telescope of the VLT. It will implement missions of indirect detection of planets by looking for footprints of planets in a dust disk, and direct detection of exoplanets. Ge et al. (1999) report on developments of two next generation ground-based very high resolution optical and IR spectrograph for sensitive exoplanet search.

An interferometry technique for imaging nearby star systems is also being developed. Hinz et al. (1999) designed a nulling interferometer and demonstrated it for the MMT (Multiple Mirror Telescope) and LBT (Large Binocular Telescope). The Terrestrial Planet Finder (TPF) is currently envisioned for an interferometer with a baseline of 75 - 1000 meter, with four-flying elements to detect and obtain spectra of exoplanets of Earth-like size. But, Angel, Burge, & Woolf (1999) consider downsized version with three elements extending over 12 meter. Integration times of approximately 7.5, 3.9 and 0.8 days would be needed to detect an Earth-like exoplanet at a distance of 10 pc.

Direct imaging technology of exoplanets, an enormous challenge, is implemented by Neuhäuser et al. (2000). Kenworthy, Hinz, & Angel

(2000) present a new detection technique which relies on the presence of a strong molecular absorption band in the thermal emission from the planetary atmosphere. The technique has a potential for the direct detection of light from an exoplanet and also the first step in performing atmospheric spectroscopy of exoplanets.

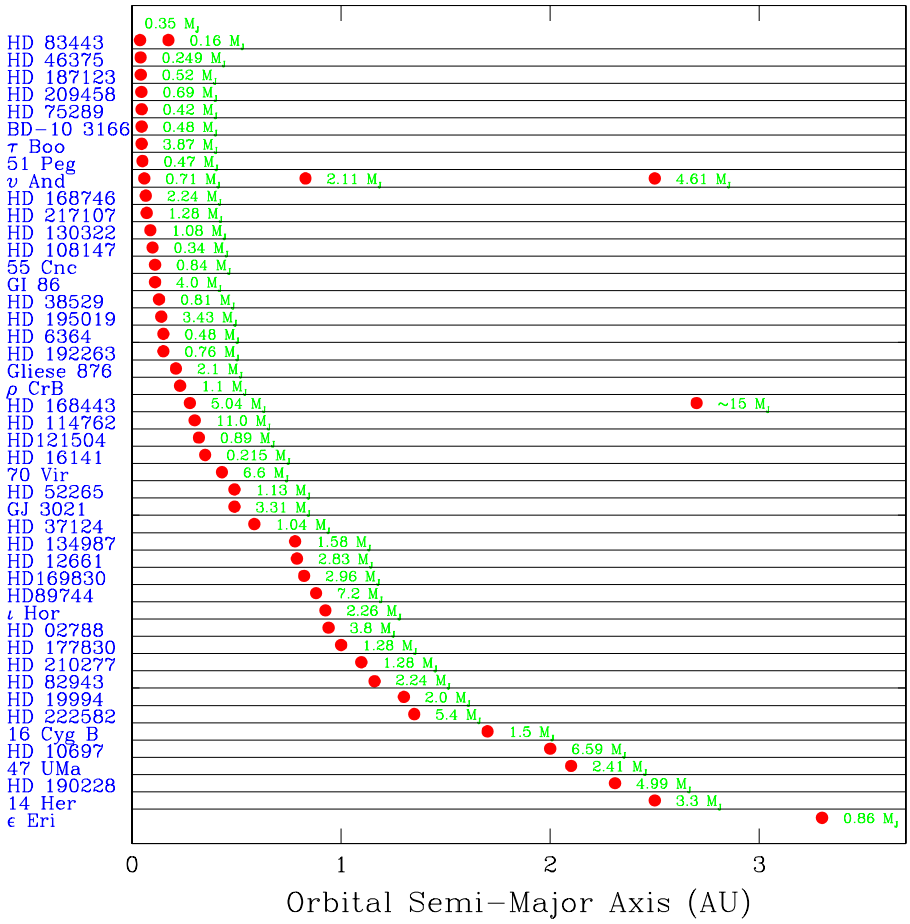

Fig. 2.1 Distribution of known exoplanets with respect to the orbital semi-major axes. The exoplanets themselves have minimum masses ($M \sin i$) between ~ 0.2 and ~ 10 M_J, orbital semi-major axes from ~ 0.04 to ~ 3.4 AU, and eccentricities as high as ~ 0.71. A total of 46 confirmed exoplanets are known as of the end of Nov. 2000.

Chapter 3

HABITABLE ZONE

3.1 Introduction

The habitable zone (HZ), or exosphere, has been discussed for many years (Huang 1959; Shklovski & Sagan 1966; Hart 1979). Recently, Kasting, Whitmire, & Reynolds (1993) have seen renewed attention. The HZ is the range of orbital distance from a star in which a planet with an atmosphere can maintain liquid water on its surface, corresponding to the temperature range from the evaporation point (373 K) to the freezing point of water (273 K). Within this limits, carbon-based organisms could sustain life.

Gehman, Adams, & Laughlin (1996) found the HZ to be 0.35 AU$\leq$ $r(L_*/L_\odot)^{-1/2} \leq$ 3.2 AU. But, this is highly optimistic interval. It represents the widest possible range of orbital radius that could conceivably allow for a habitable planet.

In the model of Kasting, Whitmire, & Reynolds (1993), interval of

the HZ was calculated to be 0.84 AU $\leq r \leq$ 1.67 AU, which was the HZ interval in a broad sense. This limit ignores the temporal evolution of the planetary system. In the timescale of current Earth's age, i.e., 4.6 Gyr, brightening of a star causes its HZ to move outward. Therefore, a conservative estimate for the width of the 4.6 Gyr 'continuously habitable zone(CHZ)' is 0.95 AU $\leq r \leq$ 1.15 AU. Within 4.6 Gyr, intelligent life have evolved from a primitive organism, and microbial life needed up to 1 Gyr to appear on the Earth.

3.2 Definition of Life

On the Earth, the age of the earliest organismic fossil is 3.5 Gyr. However, this timescale must not be thought to be the essential condition for life evolution. Life considered in this thesis comprises a lower life as well as a higher one. We may expect that the evolution of life on any planets follows that on the Earth.

In order to investigate the HZ, we may need to identify what is living and what is not. Animals, for example, are living and rocks are not. The most basic definition of life might involve the ability to ingest nutrients, to give off waste byproducts, and to grow and reproduce. The definition of what is a nutrient and what is a byproduct is difficult, since different species can utilize a wide variety of sources of energy.

We also have a problem with the concept of growth (Although moun-

tains and crystals grow by freeze or by thaw weathering, we know that these are not alive). And, after the identity of virus is revealed, it is believed that reproduction is an essential character of life. Although viruses contain DNA, they are not able to reproduce on their own. They propagate by invading cells, using the chemical machinery in that cell to produce a large number of copies of the original DNA, and then breaking apart the cell and sending the offspring out as new invader. Viruses clearly are capable of reproducing, but they cannot do so on their own. They are on the boundaries of what may be considered as living.

We need to recognize that the definition of life will be based on what we know of living and not living being that we come in contact with, and that is ambiguous. There will always be exceptions or counter-examples, and such a definition will always be determined by suite of organism that we see on the Earth today. Similarly, at the boundaries between the living and the not living, any single definition will fail (quoted from Jakosky 1998).

3.3 Climate Stabilization by the Carbonate-Silicate cycle

The relation between atmospheric CO_2 level and surface temperature was first proposed by Walker (1981, 1991). The carbonate-silicate cycle relies on heat flux in a planetary interior to drive plate tectonics and to

vent CO_2 gases stored in the crust through volcanos at plate margins. And, to keep this climate stabilizing cycle for 2 Gyr, a planet or a moon must be larger than Mars. Smaller planet or moon would lose their internal heat too quickly and would become tectonic inactive. Venus, which presumably has Earth-like heat flux, does not have plate tectonics, possibly because it does not have any water (Turcotte 1996).

With the CO_2 gases elevated, the Earth is able to keep warming out to 1.67 AU (Kasting, Whitmire, & Reynolds 1993). Carbonate-Silicate cycle is essential to our discussion of planetary habitability, so we explain in details. If the general mineral containing silicate is represented as $CaSiO_3$, atmospheric CO_2 created by a volcano reacts in following steps. The initial weathering reaction can be written as

$$\underset{\text{(calcium silicate)}}{CaSiO_3} + 2CO_2 + H_2O \rightarrow Ca^{++} + 2HCO_3^- + SiO_2. \qquad (3.1)$$

And, the dissolved products of silicate weathering are carried by streams and rivers down to where organisms use them to make shells of calcium carbonate, i.e., a shell and limestone, expressed as

$$Ca^{++} + 2HCO_3^- \rightarrow \underset{\text{(calcium carbonate)}}{CaCO_3} + CO_2 + H_2O. \qquad (3.2)$$

When the organisms die, these shells fall to the seafloor. Most dissolve on this way down, but a fraction become incorporated in carbonate sediments. The overall reaction, adding reactions (3.1) and (3.2) is expressed

as

$$\underset{\text{(weathering \& sedimentation)}}{CaSiO_3 + CO_2 \rightarrow CaCO_3 + SiO_2.} \tag{3.3}$$

Weathering reactions will remove silicate slowly. The estimated rate of silicate weathering is sufficient to remove all the carbon in the combined atmosphere/ocean system in about 0.5 Myr (Holland 1978 ; Berner, Lasaga, & Garrels 1983). So, some process must restore carbon to the system in order to maintain a steady state. The calcium silicate is reformed by carbonate metamorphism, under high temperature and pressure. And, the CO_2 is returned to the atmosphere by volcano.

$$\underset{\text{(volcano)}}{CaSiO_3 + CO_2 \leftarrow CaCO_3 + SiO_2.} \tag{3.4}$$

In reaction (3.1), if a planet or the Earth became cold enough so that the oceans froze, silicate weathering would virtually cease and CO_2 would begin to accumulate in the atmosphere. Subsequently, dense CO_2 atmosphere would form, and greenhouse would ensure. Greenhouse effect, however, would melt the ice in reality, and the atmospheric CO_2 level would begin to increase before the oceans actually freeze.

3.4 Inner and Outer Edge of HZ

In the determination of the HZ limit, the most serious problem is treatment of clouds. Two different types of clouds must be considered. The first, H_2O clouds are probably most important near the inner edge

of the HZ, which, in a warm atmosphere, tend to reduce the surface temperature by increasing albedo. The second is CO_2 clouds, which are important near the outer HZ. They, however, were ignored to simplify the reaction of an atmosphere due to the difficulties in calculating the radiative effect of the clouds.

Inner edge

The inner edge of the HZ for our solar system can be estimated from the climate model of Kasting, Whitmire, & Reynolds (1993) and Kasting (1998). In the model, H_2O adiabat was assumed in the convective region and effective solar luminosity was calculated as a function of surface temperature. Two critical values of $F/F_\odot$ (normalized solar constant to the Sun) were identified: a stratosphere becomes wet at 1.1 $F_\odot$ and the oceans evaporate entirely at 1.41 $F_\odot$. The first limit is the most relevant to the habitability problem (Kasting, Whtmire, & Reynolds 1993), but we consider the second limit of upper limit for life (see Chapter 5).

Once a stratosphere becomes wet, a diffusion restriction on the upward flow of hydrogen is overcome (Hunten 1973; Walker 1977) and hydrogen produced by water vapor photolysis can escape rapidly to space (Kasting & Pollack 1983). Kasting, Whitmire, & Reynolds (1993) demonstrated that an Earth-like planet would warm and begin to accumulate significant amounts of stratospheric water vapor if it were only 5% close to the Sun than at the present time, i.e., at 0.95 AU. This limit

is 'water loss limit'. If more warming conditions exist, a planet would experience global evaporation of oceans, followed by photodissociation of H_2O vapor and loss of H_2 to space (Kasting 1998). This point is 'runaway greenhouse limit', i.e., at 0.84 AU. Both of the calculated limits ignored the radiative effect of H_2O clouds.

Outer edge

The beginning point of CO_2 clouds formation is '1st CO_2 condensation limit', i.e., at 1.37 AU. At this limit, albedo increases by CO_2 clouds and surface cools by declining convection. At further distance, cloud-free condition occurs. Therefore, CO_2 atmosphere cools the planet by enhancing the planetary albedo, and decreases the surface temperature. Then, the surface temperature may drop below about 273 K, and the water will be frozen. This limits is called 'maximum greenhouse limit', i.e., at 1.67 AU. The outer edge of the HZ may be closer in or farther out depending on CO_2 clouds. This would control atmospheres of planets to cool or warm planetary surface (Forget & Pierrehumbert 1997).

3.5 HZ around Other Stars

The width of the CHZ around other stars depends on the lifetime of the star. The calculated main sequence lifetime of a late A type star is about 2 Gyr. Although it is not sufficient for the evolution of intelligent life, it might be sufficient time to evolve a microbe. K and M type stars

evolve slowly, which causes the boundaries of the HZ to remain fixed for a long time. Hart (1979) concludes that the CHZ disappears entirely for later stars than K0 type, corresponding to masses $< 0.85\ M_{\odot}$. The reason was that he assumed that all planets lost their reduced greenhouse gases at the same time in their evolution that an atmosphere of the Earth became oxidizing within about 2.5 Gyr after planetary formation. In his model, the lower mass star had not increased much in luminosity by this time, so their planets experienced runaway glaciation.

In terms of orbital distance, the habitability limits move outward for the Mars-sized planet and inward for the large planet (Kasting, Whitmire, & Reynolds 1993). The reason is that the atmosphere of a Mars-sized planet has a large column depth relative to planetary radius, which increases both the planetary albedo and the greenhouse effect. A large planet may have somewhat wider HZ than the small one. And, a large planet has advantages to be able to hold better onto its atmosphere over time because its stronger gravitational attraction makes it more difficult for molecules to escape. Mars even loses C, N and O from its atmosphere as well as H and He (McElroy 1972). Large planet also have higher internal heat flows and should be able to maintain tectonic activity on its surfaces for longer times.

3.6 HZ in Multiple Solar Systems

It is believed that more than 65% of stars are members of binary or multiple star systems (Duquennoy & Mayor 1991). Multiple star systems generally have not been considered for habitability due to the unstable planetary orbits. But, infrared excesses have been seen in binaries as well as in single stars (Backman & Paresce 1992). This implies that planets could form in such systems. Duquennoy & Mayor (1991) give the distribution of orbital period and eccentricity for a large group of nearby multiple star systems. Kasting, Whitmire, & Reynolds (1993) estimated that about 5% of external binaries and about 50% of internal binaries could support habitable planets in stable orbits. Here, we do not consider the habitability in these systems because they are quite complex and very uncertain.

Chapter 4

PRECONDITIONS AND STABILITY ANALYSIS OF HABITABLE EXO-MOON

4.1 Introduction

In our solar system, most planets have their moons, except Mercury and Venus, in which moon formation is considered to be disturbed by the solar wind. It is believed that the moons were formed in the regions of circumplanetary disk or captured inside the solar system. Nearly all known exoplanets until now have Jovian mass or more. Hence, these giantplanets probably are composed of gases. Considering ground-based and carbon-based organisms, habitability of these gas planet is improbable. To provide a suitable habitat for life, a planet may need to have a solid or liquid surface on which organisms might dwell and an atmosphere to protect the surface from ionizing radiation (Brack 1993). Jovian mass planets does not satisfy surface conditions for habitability. So, we will

consider moons around giant gas planets (exo-moon) for habitability.

First, we select candidate exoplanets and simply postulate conditions of exoplanet systems (section 4.2). In section 4.3, we explain mass limit for maintaining atmosphere. Section 4.4 shows dynamical stability of an exo-moon with respect to the separation between giantplanet and exo-moon. In sections 4.5, 4.6, 4.7 and 4.8, several conditions for habitable moon are calculated within the limits found in section 4.3. Problem with magnetosphere is discussed in section 4.9.

4.2 Properties of Candidate Exoplanets

In order to investigate stabilities of moons around giantplanets, we choose two candidates among the known extra-solar systems, 47 Ursae Majoris (47 UMa) detected by Butler & Marcy (1996) and ι Horologii (ι Hor) detected by Kürster (1999), which have relatively good observational data. We summarize the stellar and exoplanetary properties of 47 UMa and ι Hor systems in Table 4.1. Presently, because of technical difficulty and observational error, there are only handful of data about giantplanets and none about exo-moons. For the ease of analysis, we adopt several simplifications. First, we ignore the inclination angle of the orbital plane between giantplanet and exo-moon. Second, spin precession and spin-orbit precession are ignored. Third, in all cases, giantplanet have only one moon expect section 4.7. Fourth, initial rotation period of

giantplanet is similar to that of Jupiter. Fifth, density of ginatplanet and exo-moon are similar to that of Jupiter and the Earth. Sixth, mass and atmosphere of exo-moon are the similar to that of the Earth. Seventh, an exo-moon has strong magnetosphere.

Table 4.1 Properties of 47 UMa and ι Hor systems.

	47 UMa	47 UMa b	ι Hor	ι Hor b
Sp. type	G0 V		G0 V	
Distance[a] (pc)	14.1		15.5	
$M/M_{\odot}$	1.03[b]		1.03	
$L/L_{\odot}$	1.60		1.52	
$R/R_{\odot}$	1.22		1.097	
T_e (K)	5882		6125	
M_v	4.3		5.4	
[Fe / H]	0.01[b]		-0.12[e]	
P_{rot} (days)	21		7.9	
log g (cgs)	4.31		4.43	
log $R'HK$	-5.041		-4.65[e]	
RV (m/s)	46		67	
$v \sin i$ (km/s)	2.0			
Age (Gyr)	6[c]		6.89[e]	
a (AU)		2.11		0.925
P_{orb} (days)		1035		320
e		0.096		0.161
$M \sin \iota$ (M_J)		2.4		2.31
dist^{d}_{peri}(AU)		1.097		0.776
disp^{d}_{ap}(AU)		2.31		1.075

47 UMa is based on Henry et al. (2000) and ι Hor is based on Kürster et al. (2000); [a] derived from parallaxes in the *Hipparcos* catalogue (Perryman 1997); [b] Gonzalez (1997, 1998); [c] Assuming that 47 UMa is on the main sequence; [d] is estimated in this thesis; [e] Rocha-Pinto & Maciel (1998).

4.3 Mass Limit

There are two possible answers to the questions on volatiles of planet or moon. First, the terrestrial planets have received most of their volatiles from bombardment by comets or carbonaceous asteroids (Chyba 1990), which are formed in the outer regions of circumstellar disks and then spiraled inward (Lin, Bodeheimer, & Richardson 1996) such as Titan's atmosphere (Griffith & Zahnle 1995). Second, moons have formed in circumplanetary disk in the outer parts of a stellar nebula, which do not need for additional volatiles (e.g. Ganymede and Callisto around Jupiter).

In any case, the exo-moon must retain its volatiles for a few billion years for the emergence of life similar to the Earth. Suppose a moon has a density of 3.9 $\mathrm{g\,cm^{-3}}$, similar to Mars, an exosphere with 1000 km and temperature of 2000 K, similar to that of the Earth at solar maximum. Then, the mass must be greater than 0.07 $M_\oplus$ to retain nitrogen and oxygen for over 4.5 Gyr on the surface of the Earth. But, O_2 needed for the Earth's life can be supplied by photosynthesis and exists abundantly in the form of water. So, we can ignore loss of O_2. But, loss of N would be irreversible and could preclude the development of terrestrial life. So, a moon with Earth-like N abundance would be only marginally affected, but a moon with lower N abundance might lose their atmosphere over a long period of time. This loss process would become negligible for exo-

moons heavier than 0.12 $M_\oplus$, because the escape velocity of the N atoms is small enough. For example, Mars can lose ^{14}N efficiently, but not ^{15}N (Williams 1998).

For the long-term climate stability, about 2 Gyr timescale on the Earth, the carbonate-silicate cycle must react. This mechanism affects atmospheric CO_2 levels (see Chapter 3). For the density similar to that of Io, this yields a lower limit of about 0.23 $M_\oplus$ for an exo-moon capable of sustaining plate tectonics.

4.4 Roche - Hill's limit

For a moon around giantplanet, the moon could be broken when the tidal force exceeds cohesive force. So, there is a stable point where the force is in equilibrium. It is called the Roche limit defined as

$$d_{Roche} \equiv \alpha(\rho_M/\rho_m)^{1/3}R, \tag{4.1}$$

where ρ_M is mean density of giantplanet, ρ_m is mean density of moon and R is the radius of gaintplanet. A proportional factor α is defined 2.44 for a rigid moon.

Another limits on the orbit exists when the distance between the moon and the planet is too large. To prevent the moon from being lost by the gravitational pull of the star, moons around planets must orbit within the planet's Hill sphere, where radius is defined as

$$d_{Hill} = (M/M_s^{1/3})r, \tag{4.2}$$

where r is the separation between the planet and the star, M and M_s are masses of giantplanet and stars.

We want to examine these tidal limits for Earth-like moons around ι Hor b and 47 UMa b. Because of the lowest limit of white dwarf is 13 M_J, the beginning point of deuterium burning, we calculate up to approximately 13 M_J for M. The densities of giantplanets and moons are assumed to be those of the Jupiter and the Earth, 1.4 $\mathrm{g\,cm^{-3}}$, and 5.52 $\mathrm{g\,cm^{-3}}$, respectively. We assume 15 hours for the exo-moon's rotation period (P_0), which is similar to the rotation period of Jovian moons.

Figure 4.1 shows the resulting Roche limits and Hill's spheres of moons around ι Hor b (panel a) and 47 UMa b (panel b). We also calculate the tidal locking distance at which planet and moon become synchronized in 4.5 Gyr. Estimated tidal locking distance in both candidate systems is 136 R_J for the planetary mass of about 2.3 M_J and 245 R_J for about 13 M_J. Also specified are the innermost and outermost distances for a stable orbit regardless of the mass of giantplanet ($\sim$ 13 M_J). When a moon exists in this region, the orbit will be stable whatever the mass of the planet is.

4.5 Orbital Periods

Figure 4.2 shows possible orbital periods of moons around giantplanets, within the region of two vertical lines of Figure 4.1, for ι Hor b and

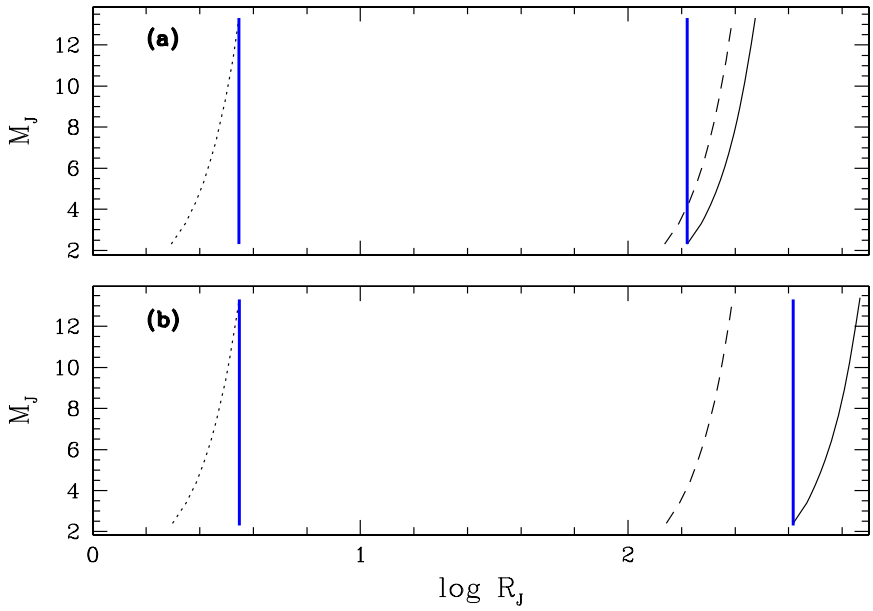

Fig. 4.1 Tidal limits of moons around ginatplanets with respect to the masses of giantplanets. Panel (a) is for ι Hor b and panel (b) is for 47 UMa b, respectively. M_J and R_J denote Jovian mass and radius. Dotted line denotes Roche limit and solid are Hill's sphere. Short dashed lines are distances at which an exo-moon becomes synchronized within 4.5 Gyr. A stable orbital region regardless of the mass of giantplanet is denoted by solid vertical lines. See text for more information.

47 UMa b. Periods are rather insensitive to the mass of the giantplanet once the mass is above about 8 M_J, and periods have little connection with that the distance is close in giantplanet. For the ground-based life, shorter period will be advantageous because of small variation of temperature.

4.6 Synchronization and Circulation Times

If a moon around a giantplanet is synchronized by tidal effect, it will make a serious influence on the habitability of the moon. If the distance between moon and giantplanet is large, the rotation period of the moon after synchronization will be long. While one side of the moon may have its atmosphere frozen, the other side may experience oversupplying radiation. The atmosphere may not be frozen if enough heat transports from the bright side to the dark side by winds. For habitability, it is desirable for the moon to rotate close to the giantplanet, but of course outside the Roche limit. Synchronization time of exo-moon is express as (Guillot et al. 1996)

$$t_{sync} \approx Q w_d (\frac{M}{m})(\frac{d^3}{Gm})(\frac{d}{r})^3, \tag{4.3}$$

where $w_d = 2\pi/P_d$ is the difference between corotation and the initial value. d the distance from a giantplanet to an exo-moon, and r the radius of exo-moon that is similar to that of the Earth. Q is the tidal quality factor of an exo-moon, defined by Goldreich & Soter (1966). The

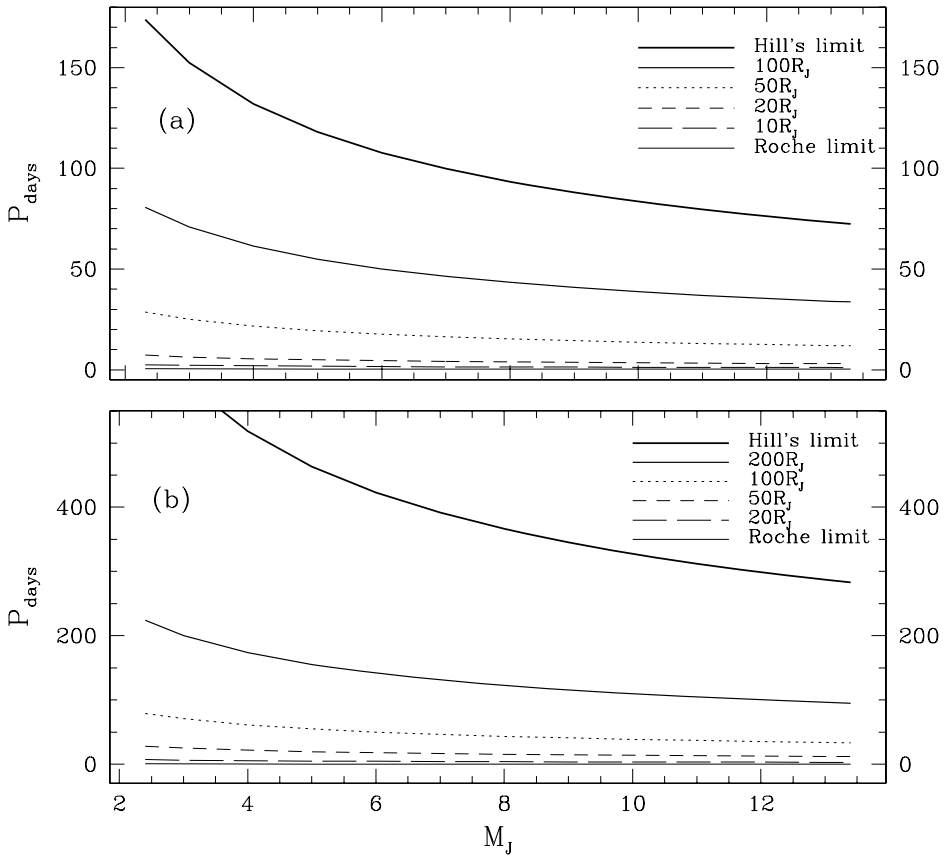

Fig. 4.2 Changes of orbital periods of moons around giantplanets with respect to the giantplanets and the separation limits (ι Hor b (a) and 47 UMa b (b)).

value of Q is in the range $10^2 \sim 10^3$ for solid, about 10^5 for Jupiter, and 10^2 for the Earth-Moon system. In case of a Jupiter-like planet around 51 Peg (0.47 M_J, 0.05 AU) rotating as fast as Jupiter, the synchronization time of the exo-moon is $t_{sync} \approx 2 \times 10^6$ yr.

Orbital periods for habitability is very important. Moons in synchronized rotations will have rotation periods equal to their orbital periods. The tidal locking radius captured by giantplanet for moons (Peale 1977) is defined as follow

$$r_T = 0.027(P_0 t/Q)^{1/6} M^{1/3}. \tag{4.4}$$

If we adopt a primordial rotation period of the Moon, P_0, to be 15 hr, t of 4.5 Gyr, and a tidal dissipation factor Q of 100, then tidal locking radius is about 96 R_J. Tidal locking radius of candidate moons within 4.5 Gyr is shown in Figure 4.1.

The tidal effect can also make the orbit circular, even after synchronization, because radial tides can dissipate energy without transferring angular momentum. The circularization timescale is (Goldreich & Soter 1966)

$$t_{circ} \approx \frac{4}{63} Q (\frac{d^3}{GM})^{1/2} (\frac{m}{M}) (\frac{d}{r})^5, \tag{4.5}$$

where Q is proportional to the tidal pumping period, that will be 10 times larger after synchronization of the exo-moon. In 51 Peg system, we calculate that the circularization timescale becomes $t_{circ} \approx 1.7 \times 10^9$ yr, which is similar to the value by Rasio et al. (1996), about 2×10^9 yr.

It is less than the age of the system, and giantplanet around 51 Peg must be circularized, which is confirmed by observation (Marcy et al. 1997).

In our calculation, we used tidal quality factor of the Earth's, 100, and initial rotation period of giantplanet similar to that of Jupiter, 15 hours. Figure 4.3 shows synchronization times of an exo-moon are proportional to M_J^{-2}. During main sequence (MS) lifetime of the star similar to the Sun, an exo-moon is synchronized regardless of the mass of giantplanet. In case of a moon at 100 R_J around 8 M_J giantplanet, an exo-moon is synchronized within 1 Gyr with $\sim$ 43 days of orbital periods. At a distance 150 R_J around 2 M_J giantplanet, synchronization for an exo-moon is not achieved during MS lifetime of the star. In this case, however, the exo-moon is not restrained by tidal force of giantplanet, and hence rotation period of the exo-moon can still be close to the initial rotation period of the exo-moon. Faster rotation causes enhanced energy exchange between a subsolar side and the opposite side, which would increase the habitability over a synchronized, slowly rotating exo-moon. However, when the difference of distance between periastron and apastron is large, an annual range in temperature will be quite large (see section 4.8 and Chapter 6).

When a moon orbits at 100 R_J around 8 M_J giantplanet, a circulation time is approximately 10^{12} yr (see Figure 4.4). Therefore, an exo-moon can not be circularized during MS phase of the star, the circularization need more than about 10^4 times the synchronization timescale.

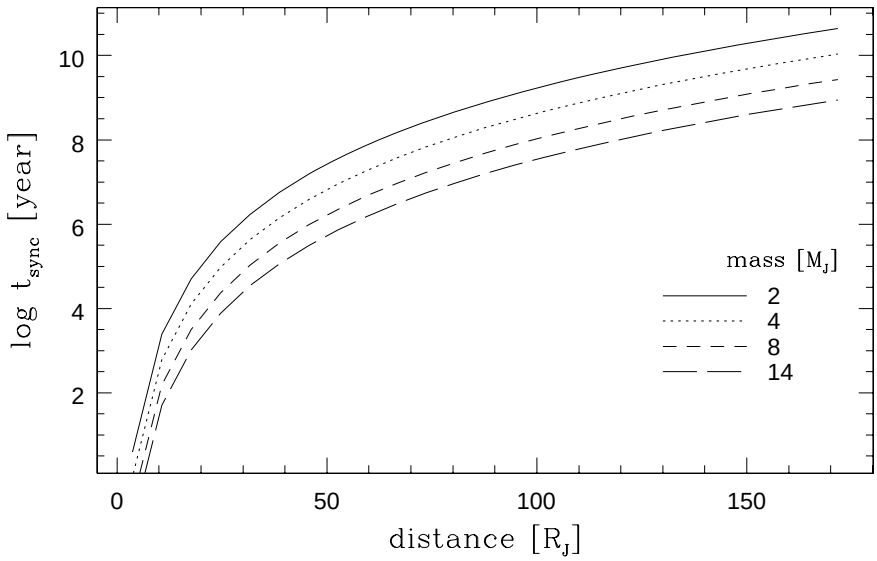

Fig. 4.3 Changes in synchronization times of moons around giantplanets with respect to masses of giantplanets and the distance from giantplanet to exo-moon. See text for more information.

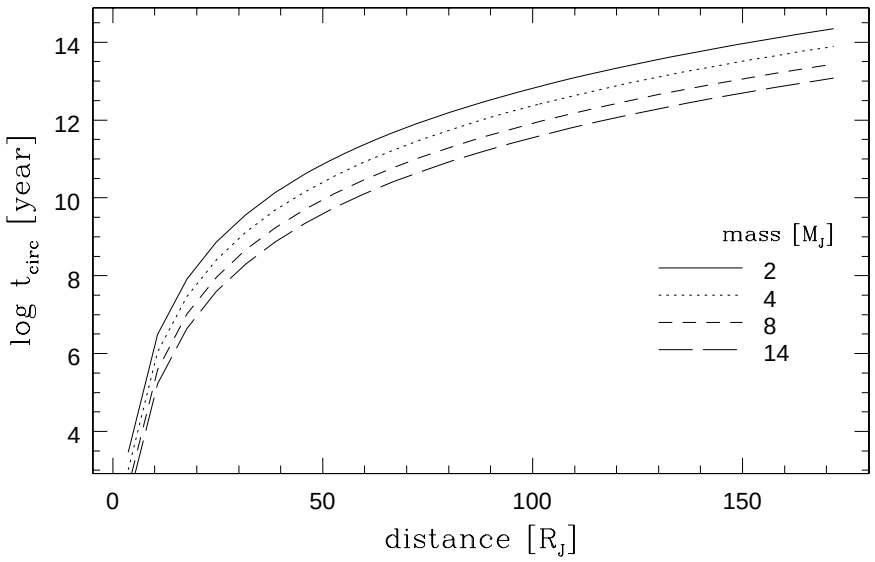

Fig. 4.4 Changes in circulation times of moons around giantplanets. See text for more information.

At a distance further than about 60 R_J from giantplanet, an exo-moon could have an eccentric orbit during MS lifetime of the star, independent of the mass of giantplanet. Therefore, beyond 60 R_J from giantplanet, an exo-moon has a chance of tidal heating by the giantplanet from the eccentric orbit, as well as short rotation periods.

4.7 Tidal Heating Rates

If the innermost moon experiences substantial tidal heating, the heating can cause tectonic process on the moon. The lower limit of the mass for self-sustaining plate tectonics is 0.23 $M_\oplus$. Io is an example whose mass is much lower than this value, yet has significant tidal heating. So, these exo-moons could remain habitable for a long period, although Io itself would not fulfill this criterion because it is too small to retain volatiles. The tidal heating rate (Peale 1979) is expressed as

$$F_{tid} = \frac{9}{19}\rho^2 n^5 R^5 e^2 (\mu Q)^{-1} \tag{4.6}$$

where n is orbital angular velocity, μ the rigidity, e the orbital eccentricity, and ρ the density of a moon. Io's eccentricity is 0.004 by a $4:2:1$ mean motion resonance with Europa and Ganymede. So, Io's tidal heating energy is calculated to be $\sim$ 41 ergs cm^{-2}sec^{-1}, perhaps enough to drive plate tectonics (Williams 1998). If several moons around exoplanets exist naturally, similar relationships might occur.

For the calculation of tidal heating rate, we adopt an exo-moon's

rigidity, μ, the same as Io's, 6.5×10^{11} dynes cm^{-2}, an exo-moon's density, ρ, the same as that of the Earth. We also consider an exo-moon's orbital angular velocity, n, with respect to the separation between exo-moon and giantplanet, in which n is changed by this separation. We calculat tidal heating rate with three cases of differing eccentricities. Figure 4.5 is the result for the orbital eccentricity, e, similar to that of Europa (e =0.01), Figure 4.6 for Io (e =0.004), and Figure 4.7 for Ganymede (e =0.0006). For each case, we calculate tidal heating rate by a giantplanet whose mass is 3 M_J, 7 M_J, and 13 M_J. We also compare the resulting tidal heating rate with that of Io, the horizontal line in the Figures. As shown in Figures, even a moon with a little eccentricity could receive significant heating. For example, even if an exo-moon orbits close to giantplanet, e.g., at 10 R_J, with eccentricity of 0.0006 (similar to Ganymede), the exo-moons can experience heating greater than that of Io, regardless of the mass of the giantplanet. Volcanic activity at the interior of Io indicates that its inside is under a high temperature and active condition. It is believed to be a direct result caused by Jovian tidal heating, which is different from the volcanos in Venus or the Earth: The energy source for these planetary volcanos is their interiors.

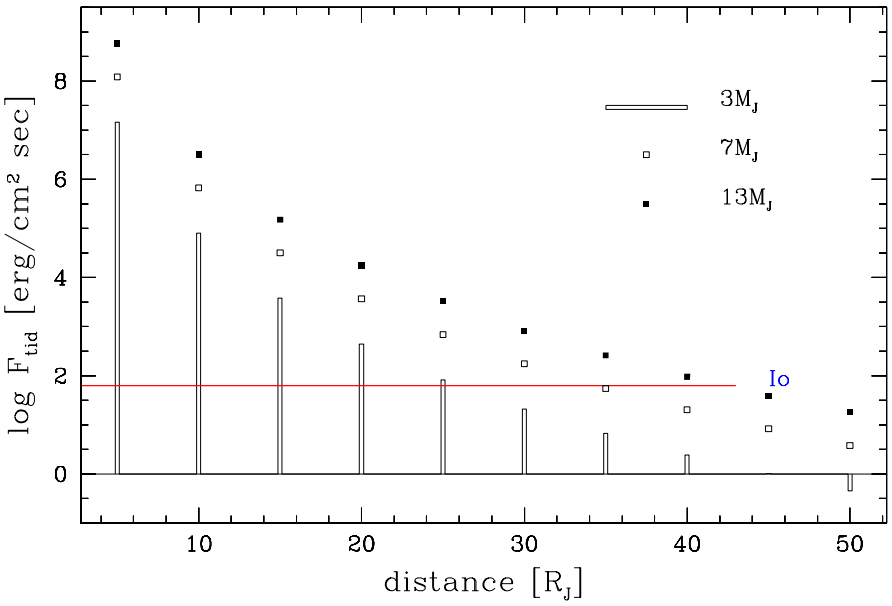

Fig. 4.5 Tidal heating rates with respect to the distance from giantplanets and the masses of giantplanets. A horizontal line denotes heating rate of Io. Assumed eccentricity is similar to that of Europa (e =0.01).

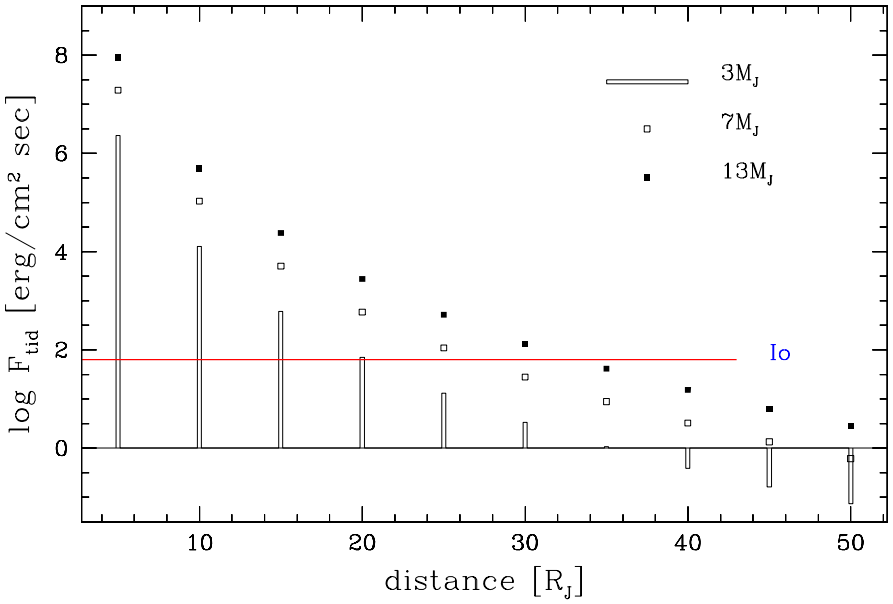

Fig. 4.6 Tidal heating rates for eccentricity of 0.004 (similar to Io).

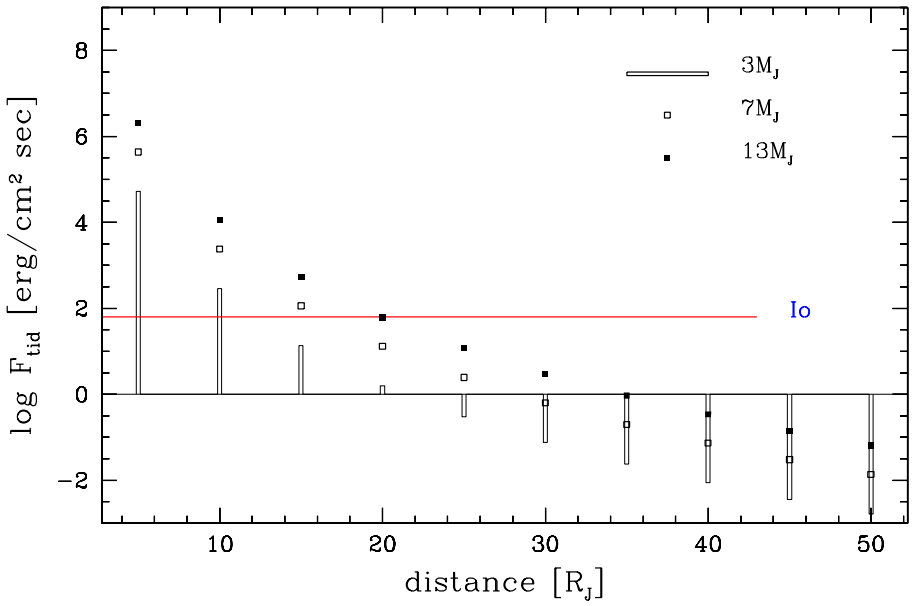

Fig. 4.7 Tidal heating rates for eccentricity of 0.0006 (similar to Ganymede).

4.8 Temperatures of Possible Exo-moons

Even though a moon can exist stable under the conditions discussed in the previous sections, a habitable exo-moon might be impossible due to inadequate temperature if a moon around a giantplanet is located too close or too far from a star, or has a high eccentricity.

There are three common definitions of temperature regarding habitability. The first definition is the effective temperature. As the temperature at the top of the planetary atmosphere, it is determined by albedo of the planet and its distance from the star.

$$T_e = \frac{(1-A)L_*}{4\pi\sigma\alpha}\frac{1}{\sqrt{r_p}} = (1-A)^{1/4}(\frac{R_*}{2r_p})^{1/2}T_* \tag{4.7}$$

where α is constant for a planetary rotation, whose value is in the range $2 \leq \alpha \leq 4$ with greater value for fast rotation. A is albedo of the moon, σ is the Stefan-Boltzman constant ($5.67 \times 10^{-8}\mathrm{W/m^2K^{-4}}$), T_* the stellar effective temperature, R_* the stellar radius and r_p the radius of the planet. The second definition is the blackbody radiation temperature, at which incoming and outgoing flux from the atmosphere of planet reach an equilibrium. It is expressed as

$$T_{bb} = (\frac{R_*}{2r_p})^{1/2}T_*. \tag{4.8}$$

The third definition, subsolar temperature suitable for slowly rotating planet, is the temperature expressed with the incident flux on the

planetary surface. This is incongruent for fast rotating planet. We must adopt it to calculate the solar constant in Chapter 5.

$$T_{ss} = (\frac{R_*}{r_p})^{1/2} T_* \tag{4.9}$$

In Figure 4.8, the maxima and minima of the three temperatures as functions of the distance of a planet from a star are shown. Maxima occur at periastron and minima at apastron.

For a moon around ι Hor b orbiting at 100 times of Jovian radius, with eccentricity ~ 0.161, the differences of temperatures between the maximum and the minimum are $\Delta T_e = 99$ K, $\Delta T_{bb} = 70$ K and $\Delta T_{ss} = 64$ K, for subsolar, blackbody and effective temperature, respectively. This difference is greater by about $\Delta T_e = 22$ K, $\Delta T_{bb} = 16$ K and $\Delta T_{ss} = 14$ K than the case with 1 R_J orbit.

The difference in the subsolar temperature between 1 and 100 times of Jovian radius from the giantplanet is $\Delta T_{ss} = 15$ K at the maximum and $\Delta = 9$ K at the minimum. Difference between at 1 R_J and at 10 R_J around giantplanet is approximately $\Delta T_{ss} = 1.5$ K at periastron and $\Delta T_{ss} = 1$ k at apastron. Therefore, for habitability, an exo-moon close to the giantplanet is favored. However, in this case the exo-moon would undergo slight drop in temperature when it enters the shadow by the giantplanet. We conclude that the orbital eccentricity is more important than the distance of a moon from the giantplanet for habitability, because we need temperature variation as small as possible during one revolution.

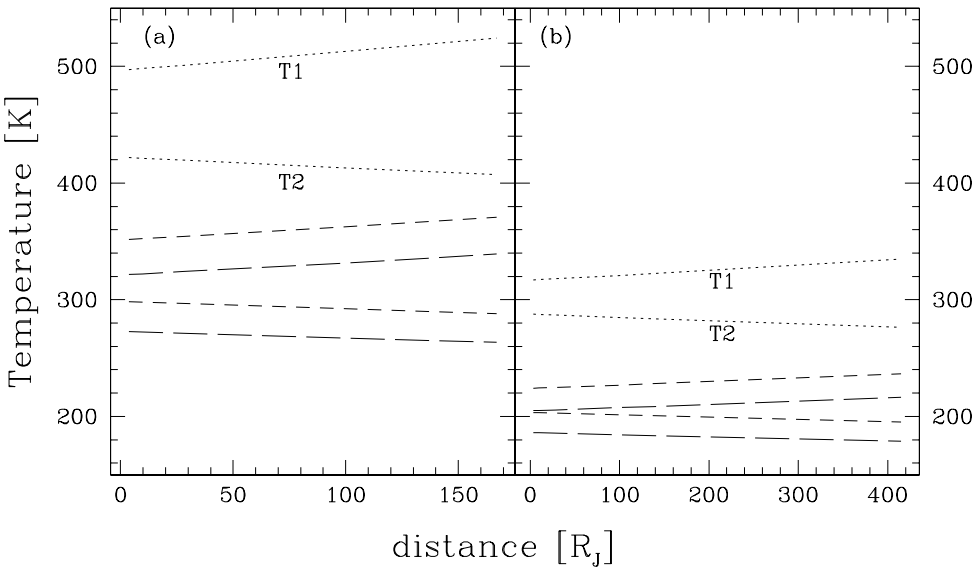

Fig. 4.8 Various exo-moon's temperatures as function of the distance from the giantplanet. Upper lines denote the temperature at periastron and lower ones the temperature at apastron from stars. Dotted lines denote subsolar temperatures, in which T1 means a maximum and T2 means a minimum. Short and long dashed lines denote blackbody and effective temperature, respectively. Panel (a) is for ι Hor and (b) is for 47 UMa.

4.9 Magnetosphere

If an exo-moon has no magnetosphere, it would undergo loss of atmosphere by electron sputtering. A moon orbiting within Jovian inner magnetosphere receives an electron flux of 4 $\times 10^8\,\mathrm{cm^{-2}sec^{-1}}$ (Van Allen 1976). This can be compared with solar wind particle flux at Mars's orbit, it receive an electron flux of 4.8 $\times 10^5\,\mathrm{cm^{-2}sec^{-1}}$, which is thought to sputter away CO_2 and O at rates of $\sim 2 \times 10^6\,\mathrm{cm^{-2}sec^{-1}}$ (Kass 1995). For example, a non-magnetized moon around Jovian-like magnetosphere could lose N at rate of $\sim 2 \times 10^9\,\mathrm{cm^{-2}sec^{-1}}$. This would deplete the Earth's N_2 within only $\sim 5 \times 10^8$ yr (Williams 1998). Titan has much more massive atmosphere than the Earth, which is composed mostly N_2. If Titan has no magnetosphere, it will lose N at a rate less than 1.2 $\times 10^7\,\mathrm{atoms\,cm^{-2}sec^{-1}}$ as a consequence of sputtering in the magnetosphere of Saturn (Strobel 1992). Titan's atmosphere is only weakly affected. Contrary to Saturn with weak magnetosphere, if higher charged particle flux exists within one of more massive giantplanet, depletion of the atmosphere on an exo-moon by sputtering will be serious.

However, if we assume an exo-moon with strong magnetic fields, atmospheric loss by giantplanetary sputtering can be eliminated. Therefore, for the existence of atmosphere of atmosphere at the surface of exo-moon, magnetic field of the exo-moon needs to be strong and that of the giantplanet needs to be weak.

Chapter 5

ANALYSIS OF HABITABILITY IN POSSIBLE EXO-MOON

5.1 Introduction

We have presented stability of moon around giantplanet and analyzed stability of two candidate exoplanets. In this chapter, by investigating temperature of exoplanets we will choose candidate habitable exoplanets and estimate possible epochs of habitability on possible exo-moons.

In order to calculate early temperature of a habitable exo-moon, we use the climate model of Kasting (2000), which considers early Earth atmospheric elements and several other parameters. First, we present change of stellar luminosity with age and show that extra-solar system maintains a stability. We use PADOVA evolution model (Bressan et al. 1993) for the change of luminosity with the stellar age. Second, using the climate model, we examine change of early moon's temperature with

respect to CO_2 mixing ratio, which is closely related to surface temperature change in the atmosphere of early moon. Finally, we estimate possible epochs in habitability of extra-solar planetary systems.

5.2 Orbital Stability of Extrasolar Planetary System

In the case of a planetary system resembling our own, planets can get close enough to the star when the star evolves to become a giant. Thus, the innermost planets could be completely engulfed inside the stellar envelope during this phase. For the Sun at the red giant branch without any mass loss, it would swell up almost, but not quite, reaching the Earth. On the asymptotic giant branch, after the exhaustion of core helium, the Sun would engulf the Earth altogether (Rasio & Ford 1996). But, stars suffer mass loss at high rates in giant and supergiant phase (Faulkner 1972; Reimers 1975). The Earth's orbit will expand by the conservation of angular momentum. According to the evolutionary model of the Sun (Sackmann et al. 1993), when the Sun's radius reach about 0.99 AU, solar mass will be reduced 0.59 $M_{\odot}$. Under this condition, the Earth's orbit will be 1.69 AU. So, the Earth will survive in this phase (Maddox 1994). In the star and giantplanet system or giantplanet and exo-moon system, the orbit is determined by the conservation of angular momentum during mass loss phase of the stellar evolution and the change of the rotation

velocity.

Star and Giantplanet system

For a star of 1 $M_{\odot}$, there is no mass loss until about 11 Gyr (PADOVA model), so there will be no change of angular momentum due to mass loss. The decrease of stellar rotation velocity can be caused by the tidal friction from giantplanets. Angular momentum is transfered from the star to the giantplanet, and the orbit of the giantplanet will expand. But, giantplanet is located at a pretty long distance from the star and both are composed of gas bodies, thus the tidal friction by giantplanet is weak. Therefore, the orbit of the giantplanet around a solar-mass star will be maintained stable during the main sequence stage of the star.

Giantplanet and Exo-moon system

For the moon orbiting a giantplanet, orbital stability will set up early because interval for synchronization need not be long (see Fig. 4.3). Tidal friction by a moon affects giantplanet, which reduces the rotational velocity of giantplanet. Angular momentum is transferred from the giantplanet to the moon and the moon moves farther out. But, contrary to the Earth-Moon system with two rocky objects, a giantplanet is composed of gas. For solid planet, the value of tidal dissipation factor, Q is in the range of $10^2 \sim 10^3$ and for gas planet, $Q \geq 10^5$. In our calculations, giantplanetary synchronization time by moon is longer than

the MS lifetime of star. Hence, we can ignore the effect of moon in the change of angular momentum of the planet. Thus, star, giantplanet, and exo-moon system will maintain a stable orbit during MS phase without change of distances among three objects.

5.3 Luminosity Change of Star

Figure 5.1 shows evolution tracks of 0.6 $M_{\odot}$ to 1.6 $M_{\odot}$ from ZAMS to hydrogen shell burning phase, calculated with PADOVA evolution models for Z = 0.02 (Bressan et al. 1993). In Figure 5.2, we show temporal change of luminosity for 1.03 $M_{\odot}$ by interpolating the evolution tracks. Metal abundances are adopted as [Fe/H] = -0.12 for ι Hor (Rocha-Pinto & Maciel 1998), 0.01 for 47 UMa (Gonzalez 1997, 1998).

To estimate current stellar ages of 47 UMa and ι Hor, we use interpolated evolutionary tracks of PADOVA model. Estimated ages generally are highly uncertain depending on the adopted methods. Age of 47 UMa determined from the mean Ca II flux from the relationship between magnetic activity and age is 6 Gyr (Henry et al. 2000). Luminosity of 47 UMa is calculated as 1.6 $L_{\odot}$ (Henry et al. 2000). Fuhrmann, Pfeiffer, & Bernkopt (1997) obtained 7.3 $\pm$ 1.9 Gyr by isochrone fitting method. Rocha-Pinto & Maciel (1998) measure a Ca II flux for ι Hor and estimate 6.89 Gyr from isochrone fitting, and current luminosity is indicated 1.52 $L_{\odot}$ (Kürster et al 2000).

But, the ages are not consistent with PADOVA model, i.e., Figure 5.2. So, we calculate current luminosities by using the distance from stars and visual magnitudes, which are observed in detail and show similarity in several data. From the luminosity, we estimate the current age by comparison to the observed luminosity (1.60 $L_{\odot}$, 1.52 $L_{\odot}$). Table 5.1 shows the luminosity change and the solar constant with respect to age. In PADOVA evolution models the Sun is about 5 Gyr old.

Table 5.1 Changes of luminosity and solar constant with respect to stellar age.

	Sun		47 UMa			ι Hor		
age[a]	age[a]	$F/F_{\odot}$	age[a]	$L/L_{\odot}$	$F/F_{\odot}$	age[a]	$L/L_{\odot}$	$F/F_{\odot}$
7.5 ago						0	0.75	0.876
6.5 ago						1.0	0.84	0.98
6.0 ago						1.5	0.89	1.04
5.0 ago						2.5	0.955	1.116
4.0 ago	1.0	0.725				3.5	1.05	1.227
3.0 ago	2.0	0.79				4.5	1.155	1.35
2.0 ago	3.0	0.84	6.0	1.32	0.296	5.5	1.259	1.47
1.0 ago	4.0	0.92	7.0	1.445	0.325	6.5	1.38	1.61
present	$\sim$ 5.0	1.0	8.0	1.6	0.359	7.5	1.52	1.777
1.0 after	6.0	1.1	9.0	2.1	0.47	8.5	1.9	2.22
2.0 after	7.0	1.197						
3.0 after	8.0	1.3						

[a] Age is Gyr unit

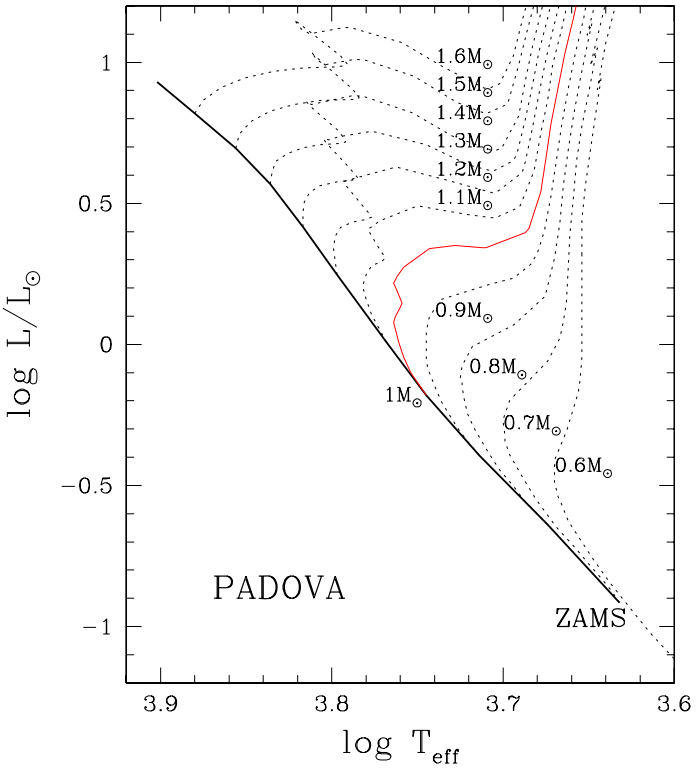

Fig. 5.1 Evolution tracks, 0.6 $M_\odot$ to 1.6 $M_\odot$, of PADOVA evolution model (Bressan et al. 1993). Thick solid line denotes ZAMS, and dotted lines are evolution tracks for various masses, expect for 1 $M_\odot$ which is denoted as a thin solid line.

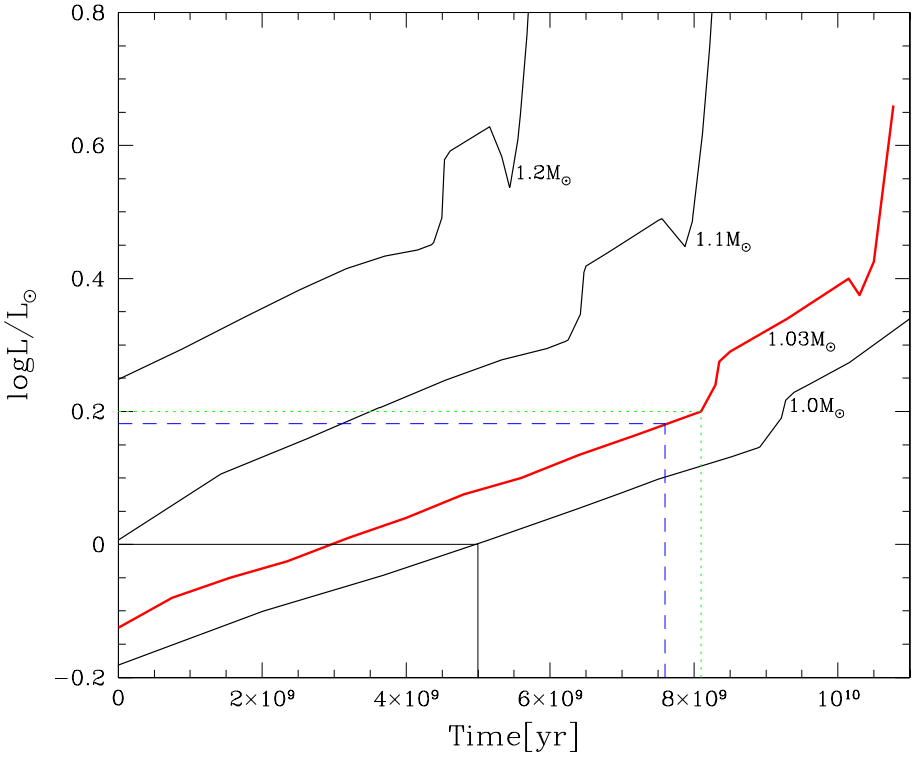

Fig. 5.2 Temporal change of the stellar luminosity in PADOVA evolution model (Bressan et al. 1993). The interpolated relation for 1.03 $M_{\odot}$ is drawn for 47 UMa and ι Hor. Dotted, short dashed and solid lines denote ages with respect to current luminosities for 47 UMa, ι Hor, and the Sun.

5.4 Temperature Profile by Early Atmospheric elements

When the Earth was formed in primitive solar nebula, light volatile matters were pushed away by solar wind, while heavy elements remained. In the subsequent stage, after experiencing impact and conjunction by primitive planetesimal continuously, gases jetted out of the ground, and atmosphere was formed. In general, current atmosphere is composed not of primitive elements but of interior elements by eruption process. At present Earth, atmosphere contains 78% of nitrogen, 21% of oxygen, 0.03% of carbon dioxide and other elements. But the atmospheres of Venus and Mars are abundant in carbon dioxide which occupies 95% of the atmosphere. This difference is in connection with the size, the temperature, and the distance from the Sun. Now, the lowest mass of particle that can remain on the surface of a planet is

$$m \geq 2.17 \times 10^{-8} \frac{R(1-A)^{1/4}}{M\sqrt{r}}, \tag{5.1}$$

where M is mass, R is radius of the planet and r is distance from the Sun. For a light particle to remain for a long time in the atmosphere, a planet must locate far away from the Sun, which means that atmospheric temperature must be low and the planet must be heavy.

Thus, the atmosphere of Earth-size planet would include more light elements than that of Venus and Mars. In the early Earth CO_2 may have been abundant, but subsequently decreased by rainfall and sunk into the

ground. As a result, a very small amount of CO_2 is detected at present. In the same context, we ignore too much CO_2 in the atmosphere of Venus or Mars, by assuming Earth-size mass and Earth-like CO_2 mixing ratio. And, evolution of life by elemental composition is another problem.

Figure 5.3 shows the altitudes, where atmosphere is considered not to exist with a low pressure of about 0.00013 atm with respect to the surface temperature. We calculate the altitude by using the early Earth climate model of Kasting (2000). In order to estimate the change of surface temperature with respect to CO_2 mixing ratio, we adopted CO_2 mixing of $0.0001\% \sim 3\%$ (Fig. 5.4). We use solar constant of 0.8 $F_\odot$ for the early Earth at 3 Gyr ago. This Figure 5.4 shows change of surface temperature (a), albedo (b) and tropospheric altitude (c). Increasing the CO_2 mixing ratio, surface temperature and tropospheric altitude become higher and albedo becomes lower. If CO_2 content increases up to 3%, in comparison to the early Earth (0.1%), early surface temperature will be higher by about 10 K. On the contrary, if it decreases down to 0.001%, early surface temperature will be lower by about 17 K.

We do not know the initial atmospheric CO_2 mixing ratio exactly, so we consider three cases: the ratio of the current Earth, 0.01% (real ratio is 0.03%), the ratio of the early Earth, 0.1%, and ten times the ratio of early Earth, 1%. As shown in Figure 5.5, in order to maintain the surface temperature of 273 K, the solar constant should be 0.64, 0.68, and 0.73 for CO_2 mixing ratios of 1%, 0.1%, and 0.01%, respectively. Namely,

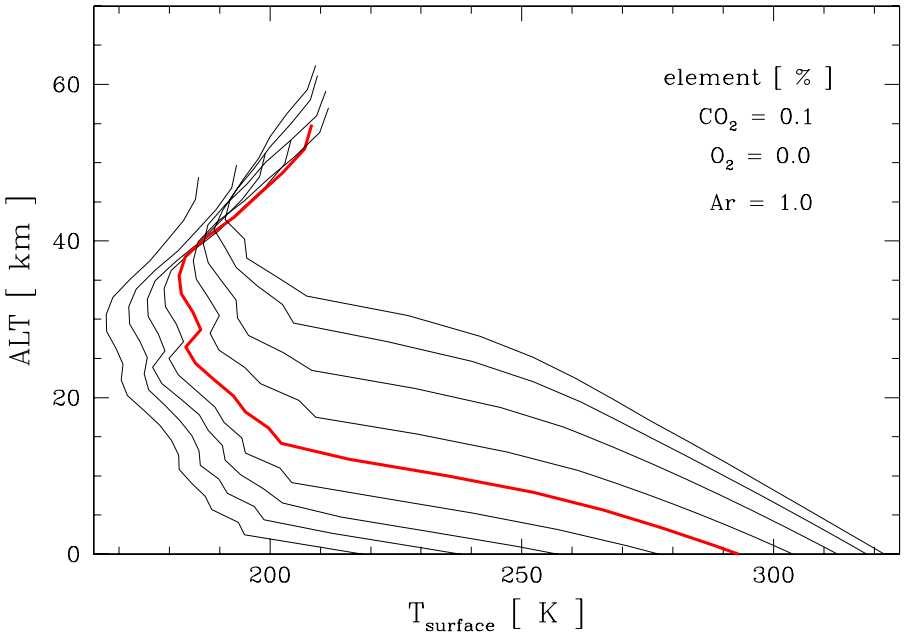

Fig. 5.3 Changes of atmospheric altitude with respect to the surface temperatures. Thick solid line is that of the early Earth at 3 Gyr. The surface temperatures are for solar constants of 0.4, 0.5, 0.6, 0.7, 0.8, 0.9, 1.0 and 1.15. We adopt the early Earth atmospheric parameters by Kasting (2000).

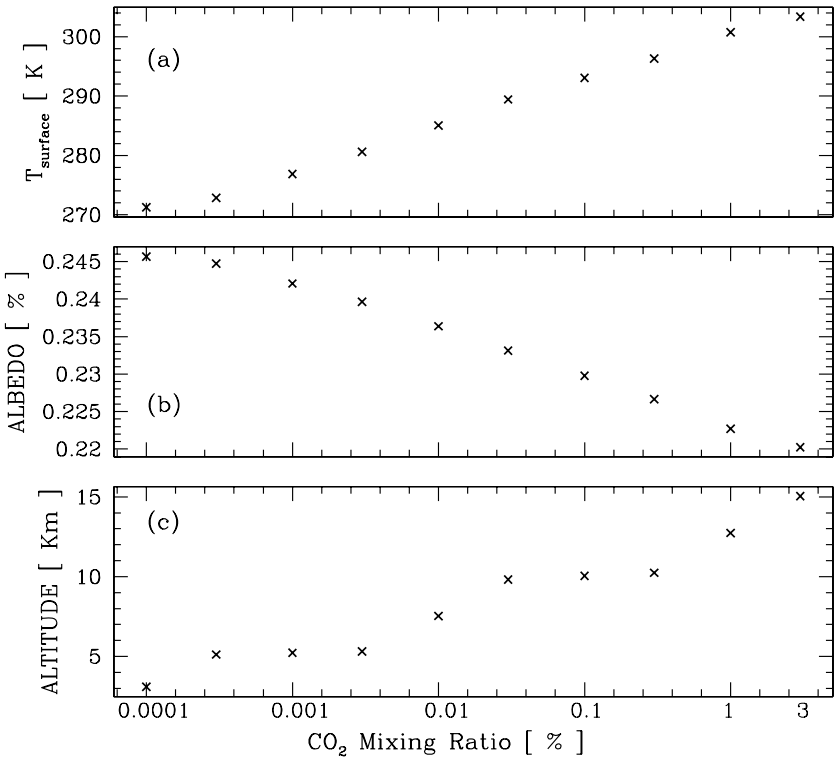

Fig. 5.4 Atmospheric conditions with respect to CO_2 mixing ratio in the early Earth, $F_\odot \sim 0.8$, at 3 Gyr ago. Surface temperature (a), albedo (b) and convective altitude (c) are shown.

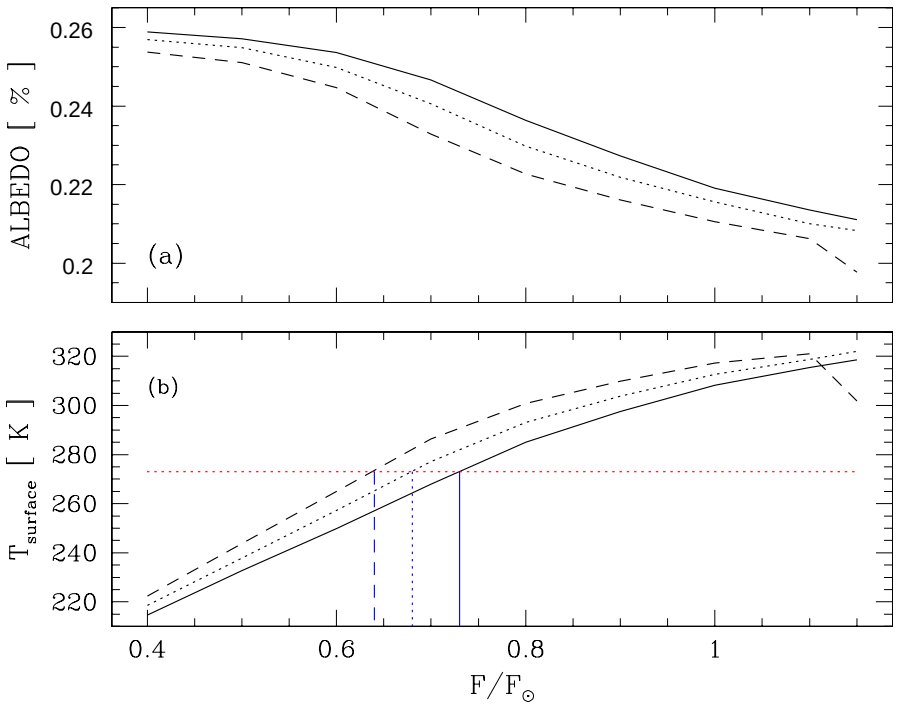

Fig. 5.5 Albedo change (a) and surface temperature change (b) with respect to the solar constant. Solid, dotted and short dashed lines are for CO_2 mixing ratio of 0.01, 0.1 and 1.0%. Vertical lines indicate 0.64, 0.68 and 0.73 $F_{\odot}$ for CO_2 mixing ratio of 1.0, 0.1 and 0.01%, which is needed to maintain surface temperature of 273 K.

surface temperature is proportional to CO_2 mixing ratio. At the top of the atmosphere where pressure is about 0.00013 atm, calculation is impossible by the climate model because convective instability is set up. In the case of CO_2 mixing ratio of 0.1%, this phenomenon appears in excess of 1.15 $F_\odot$.

5.5 Possible Epochs of habitability

By considering the temperature change of planet during the stellar lifetime, the stellar mass, and the distance between the star and the planet, we select eleven candidates among known exoplanets. We calculate the change of solar constant with respect to the stellar age using PADOVA evolution model in Figure 5.6. We consider stars of late F-type to early K-type and approximately one solar mass, and exoplanets located 0.8 AU to 2.5 AU from mother stars. Figure 5.7 shows possible epochs of habitability for the eleven candidate exoplanets. Atmospheres of the planets are assumed to contain similar atmospheric elements to those of early Earth. In the region of arrow in Figure 5.7, surface temperature ranges 273 K to 322 K, disregarding the orbital eccentricity of exoplanets.

As discussed in section 4.8, the orbital eccentricity is more important than the orbital distance for the habitability of an exo-moon. Therefore, we need to consider the orbital eccentricity and the criterion in surface

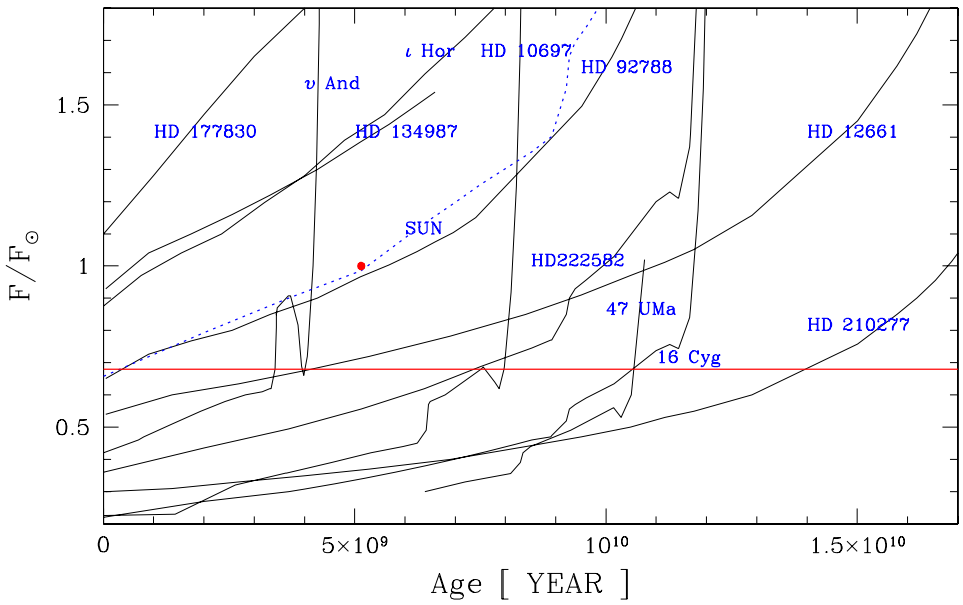

Fig. 5.6 Temporal change in solar constants, F, by adopting PADOVA evolution tracks. Parrel line is the solar constant (0.68 $F_{\odot}$) to maintain surface temperature of 273 K.

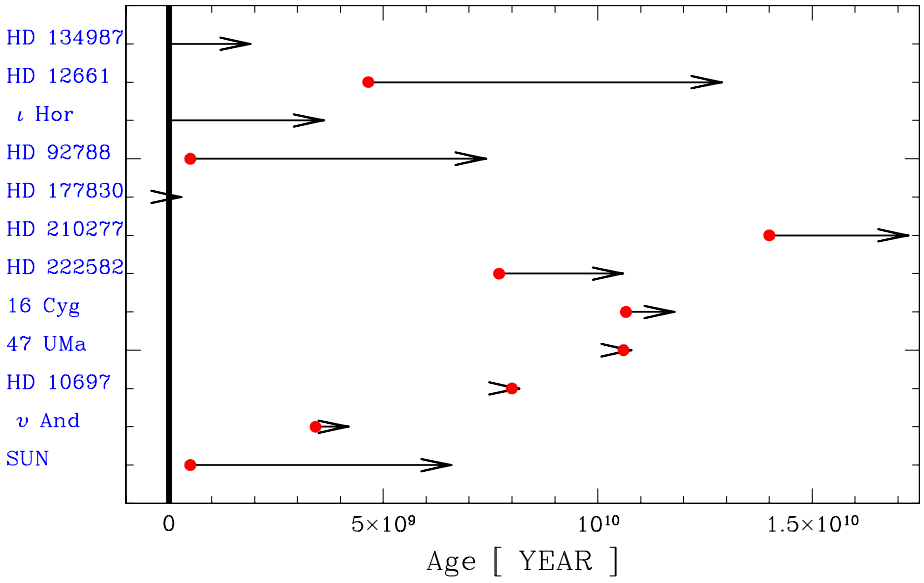

Fig. 5.7 Epochs of habitability close to exoplanets without considering orbital eccentricity. Habitable surface temperature for life is assumed as 273 K and CO_2 mixing ratio is assumed as 0.1%. Filled circle denotes starting epoch, which corresponds to 0.68 $F_\odot$ (surface temperature is 273 K), and arrow is interval to 1.15 $F_\odot$. Thick vertical line means ZAMS.

temperature for life development. Table 5.2 shows temperatures with respect to solar constant and CO_2 mixing ratio. However, it is not easy to determine the upper and the lower limit of temperature for development of life. Considering life in severely cold environment, without the possibility of migration to a mild region, lower limit is ambiguous. In general, 273 K is recognized as the lowest limit to be generated for organism. In Kasting model, because a value of 60 degree for zenith angle (an incidence angle of 30 degree) is used without concerning latitudes in global region, calculated surface temperature is a mean temperature. Currently, even if 288 K is the mean temperature on the surface of the Earth, a difference of several tens of degree exists between the equatorial and the polar region.

Table 5.2 Changes of solar constants for upper and lower limit of temperatures.

$F/F_\odot$	CO_2 ratio (%)	$T_{ss}(K)^a$	$T_{bb}(K)^b$	$T_{sur}(K)^c$
0.53	0.1	337	238	243
0.64	1	353	249	273
0.68	0.1	358	253	273
0.73	0.01	365	258	273
1.0	0.1	395	278	312.7
1.15	1	409	289	unstable
1.15	0.1	409	289	322
1.15	0.01	409	289	318.6
1.41		430	310	?
3.17		527	373	?

[a] is subsolar temperature; [b] is blackbody radial equilibrium temperature; [c] is surface temperature (calculated by using Kasting climate model)

At the equator, temperature is higher than the mean value by about 30 K. Thus, although it is not the absolute limit, we assume that the mean surface temperature of 243 K is the lower limit for the development of life, with corresponding solar constant of 0.53 $F_{\odot}$.

The solar constant of 3.17 $F_{\odot}$, for which is the blackbody radiative equilibrium temperature becomes 373 K, can be adopted as the upper limit for life generation. We also consider 'Runaway Greenhouse Limit', 1.41 $F_{\odot}$ (see section 3.3).

Figure 5.8 shows differences in solar constant from periastron to apastron for eleven candidates, calculated assuming CO_2 mixing ratio of 0.1%. Because HD 222582 b and 16 Cyg have eccentricity of 0.71 and 0.68, difference in solar constant is large. We think that there is no possibility of an organic life at the moons around these giantplanets. The range from 0.53 $F_{\odot}$ to 3.17 $F_{\odot}$ contains the possible candidates of habitability. They are HD 134987, ι Hor, 47 UMa, and HD 10697.

Ultimate candidates and time intervals of habitability is shown in Figure 5.9. Table 5.3 show the properties of four final candidates of habitability. For these candidate stars, visible magnitude and distance are known from observation. So we can derive their current luminosities. Comparing this value to the value from isochrone fitting method in Figure 5.2, current stellar ages are estimated (last row in Table 5.3). They range from 6.5 to 8 Gyr.

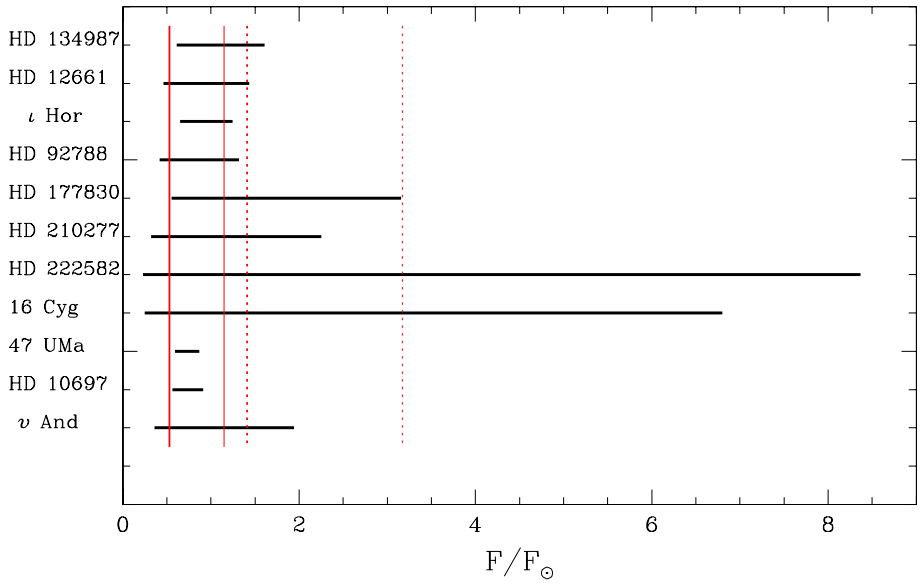

Fig. 5.8 Intervals of change in solar constant on exoplanets from periastron to apastron. Thick solid vertical line denotes lower limit (0.53 $F_{\odot}$) and thin solid vertical line denotes 1.15 $F_{\odot}$, which is upper solar constant by Kasting model. Thick dot vertical line means runaway greenhouse limit (1.41 $F_{\odot}$) and thin dot line means 3.17 $F_{\odot}$, which can be assumed upper limit because there is no standard.

Table 5.3 Properties of possible habitable candidate.

	HD 134987[a]	ι Hor[b]	47 UMa[c]	HD 10697[a]
sp. type	G5 V	G0 V	G0 V	G5 IV
$M/M_\odot$	1.05	1.03	1.03	1.10
$L/L_\odot$	1.34	1.52	1.60	2.63
a (AU)	0.81	0.925	2.11	2.12
e	0.24	0.161	0.096	0.12
[Fe / H]	0.23	-0.12	0.01	0.15
$M \sin \iota$ (M_J)	1.58	2.31	2.4	6.35
Z	0.034	0.015	0.02	0.028
Age (Gyr)[d]	8	7.5	8	6.5

[a] Vogt et al. (2000); [b] Kürster (2000); [c] Henry et al. (2000); [d] Age estimated in this thesis.

5.6 Summary

We select candidate extra-solar systems thru the habitability criterion on the temperature, and estimate their luminosity change with respect to eccentricity. We find four candidate extrasolar systems of habitability. That is, in the course of stellar evolution, organisms might appear during the habitable epoch (arrow bars plus dotted lines in Figure 5.9).

Figure 5.10 is the same as Figure 5.9, but now with age scale relative to the Sun. 47 UMa and HD 10697 show that possible habitable environment would be feasible after approximately 2.5 Gyr and 1.4 Gyr, respectively. In our calculation, however, duration for possible condition will be supported only for 0.4 Gyr, within which organisms development might be impossible, judging from life on the Earth. Especially, ι Hor

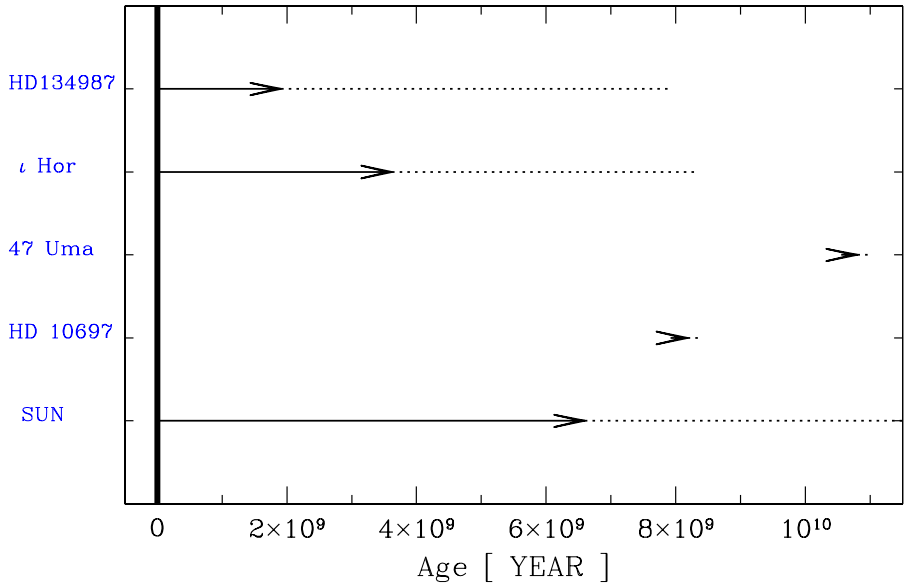

Fig. 5.9 Possible epochs of habitability in exoplanets. Arrow bar denote from beginning to 1.15 $F_{\odot}$ at semi-major axis. Dotted lines denote interval to upper limit of possible habitability with solar constant of 3.17 $F_{\odot}$. Epochs for 47 UMa and HD 10697 are shorter than the length of the arrow.

shows an interesting result. At current age, although it is the optimistic view, possible habitability among known exoplanets might exist around ι Hor b. So, we can consider a moon around a giantplanet, ι Hor b. As explained in section 4.8, if an exo-moon is located close to a giantplanet, temperature variation due orbital distance change will not be large. Assuming an Earth-size moon at 10 R_J around ι Hor b, T_{ss} are 498.5 K at periastron and 421 K at apastron. Difference of temperatures between at 1 R_J and at 10 R_J around ι Hor b becomes approximately $\Delta T_{ss} = 1.5$ K at periastron and $\Delta T_{ss} = 1$ K at apastron. Therefore, an exo-moon close to ι Hor b is desirable for habitability. We conclude that the orbital eccentricity is more important for habitability than the distance of an exo-moon from the exoplanet.

If an Earth-size exo-moon at 10 R_J around ι Hor b, although eccentricity of 0.0006 the same as that of Ganymede, the exo-moon can generate more energy than ~ 41 ergs cm^{-2}sec^{-1} of Io, i.e., ~ 288 for 13 M_J, ~ 2393 for 7 M_J, and ~ 11250 ergs cm^{-2}sec^{-1} for 3 M_J, perhaps enough to drive plate tectonics. In this case there may exist more moons than one. At this distance, synchronization is rapid, which is about 2 $\times 10^3$ yr for 2 M_J, about 4 $\times 10^2$ yr for 4 M_J and 40 yr for 12 M_J, and orbital periods of the exo-moon is about 1.1 days for 13 M_J and about 2.6 days for 2.3 M_J. For the reasons stated above, the convection mechanism of the exo-moon will differ little from that of the Earth. If the Earth-size moon in 100 R_J, synchronization becomes rapid as compared

with lifetime of MS, which is $\sim 1.85 \times 10^9$ yr, with the orbital period of exo-moon of 34 days for 13 M_J and $\sim$ 81 days for 2.3 M_J. After synchronization time, because orbital period and revolution period are similar, possible of habitability of the exo-moon will be determined by convection mechanism rather than by the stellar radiation energy. Starlit atmosphere is heated faster and higher, and the opposite side of starlit surface will become cooler, without heat convection. But, at present circumstances, the cycle of convection is not known.

In calculation by Kasting, Whitmire, & Reynolds (1993), ocean evaporates entirely at 1.41 $F_\odot$ via runaway greenhouse, which is significantly less than 3.17 $F_\odot$ considered as the upper limit on F in this work. Ground-based life is not possible then. But, we don't think even this case is entirely outside the habitability, considering the possibility of life development before the runaway greenhouse, and the possibility of underground-based organism.

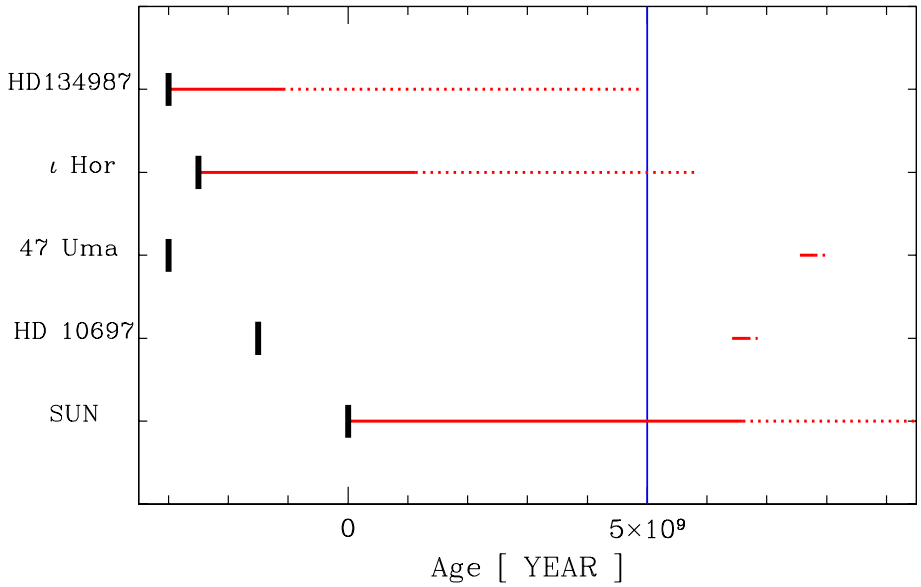

Fig. 5.10 Possible epochs of habitability in exoplanets with respect to the current age. Solid plus dotted horizontal lines denote the possible duration of habitability in each star. The length of solid horizontal lines denotes the duration calculated by Kasting model (2000) at the semi-major axis. Short vertical lines denote ZAMS of the stars. The origin of the age is relative to the zero age of the Sun and the current solar age is adopted as 5 Gyr.

Chapter 6

DISCUSSION

The idea of SETI was first introduced by Cocconi & Morrison (1959). In this paper, they discussed the possibility of the existence of ET (Extraterrestrial) and detecting methods. At the same time, an American astronomer Frank Drake attempted the first SETI, named Project Ozma. The project scanned for signals from τ Ceti and ϵ Eri over two weeks, without detecting any meaningful signal. This is the opening of SETI.

Despite the efforts for more than forty years the project Ozma, no ET signal has been detected. However, the null result must not be interpreted as the evidence against ET. A hopeless and hopeful truth is that we can never prove that we are the unique being. And, a large amount of technical and scientific development will be accomplished thru SETI even when it fails. New understandings of several astronomical phenomena and improvements of computer science in analysing software and hardware are achieved.

Drake equation was developed by Frank Drake in 1961 as a way to focus on the factors which determine how many intelligent, communicating civilizations there can be in our galaxy. The Drake Equation is defined as

$$N_{ETI} = N_* f_s N_p f_e f_l L \tag{6.1}$$

where N_{ETI} is the present number of communicating civilizations in our Galaxy and each symbol denotes

N_* : Number of stars in the Galaxy,

f_s : Fraction of sunlike stars,

N_p : Average number of planets per star,

f_e : Fraction of planets suitable for life,

f_l : Fraction of those planets where life actually develops,

f_i : Fraction of planets with life where intelligent civilizations arise,

L ; (Lifetime of civilization with ability and desire to communicate) / (Lifetime of Milky Way galaxy).

The factors in this equation are almost impossible to determine with any certainty. However, with investigations in astronomy, biology, geology, and other sciences, we will be able to make better estimates. Similarly, we can think of probability of habitable exo-planets defined as

$$N_{ep} = N_* f_s N_p f_e. \tag{6.2}$$

It provides the number of habitable exoplanets in our galaxy. In

this thesis, we focused on f_e and f_l. The first question for the detected exoplanets will be 'Are these suitable for life ?' Ultimate, purpose of detecting exoplanets is the search for ETI. We may think that detecting exoplanet is an intermediate road to SETI.

Since all exoplanets discovered so far are probably composed of gases, they are not suitable for ground-based organisms. Therefore, we consider possible Earth-like moons around giantplanets, and we investigate development and habitable environments of ground-based life.

In case of an Earth-like moon around giantplanet orbiting in the range of Roche and Hill's limit, an exo-moon can be maintained in stable orbit during MS phase of the star. Some moons around exoplanets might be habitable, but only if they are properly sized. An 0.12 $M_\oplus$ exo-moon in an Io-like orbital resonance which has a Ganymede-like magnetic field, could conceivably remain habitable for billions of years (Williams 1998). However, we could not determine the upper limit of the mass in case of a rocky exoplanet or an exo-moon due to ambiguous criteria for a rocky planetary degeneration.

A synchronization time for an exo-moon changes with respect to the distance from a giantplanet. We estimate that at the distance more than about 60 R_J from a giantplanet an exo-moon would have an eccentric orbit during MS phase of the star because the exo-moon is not restrained by the tidal force of giantplanet regardless of the mass of giantplanet. Therefore, beyond 60 R_J from giantplanet, the exo-moon has a chance of

tidal heating by the eccentric orbit as well as short rotation periods. Even close-in exo-moons with mass less than 0.23 $M_{\oplus}$, the lower limit for sustaining plate tectonics, could conceivably form an atmosphere with high temperature. We estimate that, even with eccentricity of 0.0006, similar to that of Ganymede, an exo-moon at 10 R_J around a giantplanet could receive more heat than that of Io, i.e., $6.5 \times 10^{11}\,\mathrm{dynes\,cm^{-2}}$, regardless of the mass of giantplanet. Unfortunately, we do not know the atmospheric influence on tidal heating for exo-moons more massive than 0.23 $M_{\oplus}$. Additional energy may be unnecessary in this case.

According to our calculation of orbital stability of exoplanetary system, star, giantplanet, and exo-moon system will maintain a stable orbit during the MS lifetime of the star without the change of separation between them.

The climate model of Kasting (2000) shows the change of a surface temperature in the early Earth with respect to atmospheric elements. We assume the range $0.01\% \sim 1\%$ of CO_2 to estimate early temperature on the surface of an exo-moon. However, the climate model is incapable of dealing with an exo-moon similar to Venus or Mars, or a solar constant larger than 1.15 $F_{\odot}$. So, we can not calculate the upper limit of temperature for development of organism. Hence, we calculate the range of upper limit at 3.17 $F_{\odot}$, which coincides with a blackbody temperature of 373 K.

Among forty-six exoplanets discovered so far, we selected four can-

didates. Using PADOVA evolution models (Bressan et al. 1993), we calculate the luminosity changes and the orbital stability with respect to the stellar age, and set up a criterion for habitable temperature by using the early Earth climate model (Kasting 2000). We estimate possible epochs and duration of habitability for the candidates.

To be optimistic, it is possible that a habitable exo-moon may exist around ι Hor b. In our result, an adequate environment might formed already about 7.5 Gyr ago when ι Hor began its MS life. Moreover, the environment for a life development have been maintained since that time.

For the suitable temperature to be maintained for life development and habitability, an orbital eccentricity of giantplanet is more important than the orbital separation between the giantplanet and the exo-moon. For example, about 1.85×10^9 yr is needed for synchronization of a moon at 100 R_J around a giantplanet. In this case the rotation period becomes approximately $34 \sim 81$ days. There are the possibility of convection mechanisms that can diminish the diurnal range by the circulation of energy i.e., in the very slow rotating moon. Similarly, the annual range in highly eccentric orbit could be diminished. For example, an exo-moon at 10 R_J around ι Hor b with 0.161 of eccentricity, has a gap of 77.5 K between the maximum and the minimum temperature. We believe that convection should be studied in detail for life development and habitability.

Currently, only one study on the exo-moon can be found in the lit-

eratures. Williams (1998) outlines the stability of an exo-moon. Thus, there are many unanswered questions for the exo-moon. For example, how does the surface temperature change by convection mechanism? In the climate model by Kasting (2000), there is no information for subsolar side and the opposite side because he does not consider the rotation of the Earth. Also, if an exoplanet is more massive than 13 M_J, how much energy is transferred to an exo-moon by deuterium burning in the exoplanet? When a moon revolves exoplanet with a high eccentricity, is there a possibility of underground-based or undersea organisms?

Our investigation so far on the possibility of life development and habitability around the exoplanets considered 'moons around giantplanets' only. In fact, there can be not only 'moons (satellites)' but 'rocky planets' such as the Earth. In the near future, a 'planet' similar to our planet will no doubt be detected, and then 'the planet' will be probed directly in the search for a life.

REFERENCES

Angel, R., Burge, J., and Woolf, N. 1999, Flat mirror optics to study extra-solar terrestrial planets from space. in Working on the Fringe: Optical and IR Interferometry from Ground and Space. eds. S. Unwin & R. Stachnik, p339

Backman, D. E., and Paresce, F. 1992, Main sequence stars with circumstellar solid material: The Veg phenomenon. In Protostars and Planets III, Univ. of Arizona Pres, Tucson.

Baranne, A., Queloz., Mayor, M., et al. 1996, ELODIE: A spectrograph for accurate radial velocity measurements. A&AS, 119, p373-390.

Barshay, S. S., and Lewis, J. S. 1976, Chemistry of primitive solar material. ARA&A, 14, p81-94.

Bennett, D. P., Rhie, S. H., Becker, A. C., Butler, N., et al. 1999. Discovery of a planet orbiting a binary star system from gravitational microlensing. Nature 402, 57-59.

Berner, R. A., Lasaga, A. C., and Garrels, R. M. 1983, The carbonate-silicate geochemical cycle and its effects on atmospheric carbon dioxide over the past 100 million years. Am. J. Sci. 283, 641-683.

Borucki, W. J., Koch, D. G., Lissauer, J. J., et al. 1998, Detection of Extrasolar Planets by Transit Photometry in the Antarctic. American Astron. Soc. Meeting

Boss, A. P. 1995, Proximity of Jupiter-like planets to low-mass stars. Science 267, 360-362.

Boss, A. P. 1996a, Extrasolar planets. Physics Today 49, 32-38.

Boss, A. P. 1996b, Giant planets and dwarfs meet in the middle. Nature 379, 397-398.

Brack, A. 1993, Liquid water and the origin of life. Orig. of Life and Evol. of Bios. 23, 3-10.

Bressan, A., Fagotto, F., Bertelli, G. and Chiosi, C. 1993, Evolutionary sequences of stellar models with new radiative opacities. II Z=0.02. A&AS, 100, 647-664.

Brown, T. M. 2000, Using Transits to Find and Characterize Extrasolar Planets. in Planetary Systems in the Universe, IAU Symp. no. 202

Butler, R. P., Marcy, G. W. 1996, A planet orbiting 47 Ursae Majoris. ApJ, 464, L153-L156.

Butler, R. P., Marcy, G. W., Williams, E., Hauser, H., and Shirts, P. 1996, Three new "51 Pegasi-type" planets. ApJ, 474, L115-L118.

Charbonneau, D., Brown, T. M., Latham, D. W., and Mayor, M. 2000, Detection of Planetary Transits Across a Sun-like Star. ApJ, 529, L45-L48.

Chyba, C. F. 1990, Impact delivery and erosion of planetary oceans in the early inner Solar System. Nature 343, 129-133.

Deeg, H. J., Martin, E., Schneider, J., et al. 1997, The TEP Network - A Search for Transits of Extrasolar Planets : Observations of CM Draconis in 1994. A & AT, 13, 233-243.

Dunham, E. W. 1999, Detection Of Extrasolar Planets Using Spaceborne Transit Photometry. in Bioastronomy 99: A New Era in Bioastronomy. 6th Bioastronomy Meeting-Kohala Coast Hawaill.

Duquennoy, A., and Mayor, M. 1991, Multiplicity among solar-type stars in the solar neighborhood. II. Distribution of the orbital elements in an unbiased sample. A& A, 248, 485-524.

Edvardsson, B., Andersen, J., Gustafsson, B., Lambert, D. L., Nissen, P. E., and Tomkin, J. 1993, The Chemical Evolution of the Galactic Disk -

Part Two - Observational Data. A&AS, 102, 603E.

Erskine, D., and Ge, J. 1999, A Prototype Fringing Spectrograph for Sensitive Extra-solar Planet Searches and Astroseismology studies. American Astron. Soc. Meeting

Esquerdo, G. A. 1998, A Photometric Search for Extra-Solar Planets: The Prototype System and Early Results. American Astron. Soc. Meeting

Faulkner, D.J. 1972, Evolution of nuclei planetary nebulae. Astron. Soc. Aust.,2, 272.

Ford, E. B., Rasio, F. A., and Sills, A. 1999, Structure and Evolution of Nearby Stars with Planets. I. Short-Period Systems. ApJ, 514, 411-429.

Forget, F., and Pierrehumbert, R. T. 1997, Warming early Mars with carbon dioxide clouds that scatter infrared radiation. Science 278, 1273-1276.

Fortney, J. J., Hubbard, W. B., Burrows, A., Lunine, J. I., et al. 2000, Theoretical Model of the Transit of Planet HD 209458b. American Astron. Soc. DPS meeting.

Fuhrmann, K., Pfeiffer, M. J., and Bernkopf, J. 1997, Solar-type stars with planetary companions : 51 Pegasi and 47 Ursae Majoris. A&A, 326, 1081-1089.

Gatewood, G. 1996, Lalande 21185. Bull. American Astron. Soc. 28, 885.

Gaudi, B. S. 2000, Planetary Transits toward the Galactic Bulge. ApJ, 539, L59-L62.

Ge, J., Ciarlo, D., Kuzmenko, P., et al. 1999, Next Generation Ground-based Very High Resolution Optical and Infrared Spectrographs for Extra-solar Planet Searches. American Astron. Soc. Meeting

Gehman, C. S., Adams, F. C., and Laughlin, G. 1996, The Prospects for Earth-Like Planets within Known Extrasolar Planetary Systems. PASP, 108, 1018-1023.

Goldreich, P., and Soter, S. 1966, Q in the Solar System. Icarus 5, 375-389.

Gonzalez, G. 1997, The stellar metallicity-giant planet connection. MNRAS, 285, 403-412.

Gonzalez, G. 1998, Extrasolar Planets and Metallicity. American Astron. Soc. 193.

Griffith, C. A., and Zahnle, K. 1995, Influx of cometary volatiles to planetary moons: the atmospheres of 1000 possible Titans. J. Geophys. Res. 100, 16907-16922.

Guinan, E. F., McCook, G. P., Wright, S., and Bradstreet, D. H. 1997, Photometric Searches for Planets: Evidence of a Transit Eclipse by a Jupiter-size Planet Orbiting the Eclipsing Binary CM Draconis. in Detection and Study of Planets Outside the Solar System, 23rd IAU meeting.

Guillot, T., Burrows, A., Hubbard, W. B., Lunine, J. I., and Saumon, D. 1996, Giant planets at small orbital distances. ApJ, 459, L35-L38.

Hart, M. H. 1979, Habitable zones about main sequence stars. Icarus 37, 351-357.

Henry, G. W., Marcy, G., Butler, R. P., and Vogt, S. S. 1999, A Transiting "51 Peg-like" Planet. ApJ, 529, L41-L44.

Henry, G. W., Marcy, G., Butler, R. P., and Vogt, S. S. 1999, HD 209458. IAU Circ. 7307.

Henry, G. W., Baliunas, S. L., Donahue, R. A., Fekel, F. C., and Soon, W. 2000, Photometric and Ca II H and k Spectroscopic Variations in Nearby Sun-like Stars with Planets. III. ApJ, 531, 415-437.

Hinz, P. M., Angel, J. R., Woolf, N. J., Hoffmann, W. F., et al. 1999, Imaging Extra-solar Systems from the Ground: The MMT and LBT Nulling Interferometers. in Working on the Fringe: Optical and IR Interferometry from Ground and Space. eds. S. Unwin & R. Stachnik. p401

Holland, H. D. 1978, The Chemistry of the Atmosphere and Oceans, (John Wiley & Sons, Inc., New York).

Huang, S.-S. 1959, Occurrence of life in the universe. Sci. Amer. 47, 397-402.

Huang, S.-S. 1960, Life outside the Solar System. Sci. Amer. 202, 55-63.

Hunten, D. M. 1973, The escape of light gases from planetary atmospheres. J. Atmos. Sci. 30, 1481-1494.

Jakosky, B. M. 1998, The Search For Life on Other Planets. Cambridge Univ. Press. Chapter 6.

Jenkins, J. M., Koch, D. G., Borucki, W. J., et al. 2000, Key Steps in Processing CCD Photometric Data to Detect Transits of Earth-Size Planets. American Astron. Soc. DPS meeting.

Jha, S., Charbonneau, D., Garnavich, P. M., et al. 2000, Multicolor Observations of a Planetary Transit of HD 209458. ApJ, 540, L45-L48.

Kasting, J. F., and Pollack, J. B. 1983, Loss of water from Venus. I - Hydrodynamic escape of hydrogen. Icarus 50, 479-508.

Kasting, J. F., Whitmire, D. P., and Reynolds, R. T. 1993, Habitable Zones around Main Sequence Stars. Icarus 101, 108-128.

Kasting, J. F. 1998, Habitable Zones Around Stars and the Search for Extraterrestrial Life. Amer. Astron. Soci. Meeting

Kasting, J. F. 2000, *private communication*.

Katz, D., Soubiran, C., Cayrel, R., Adda, M., and Cautain, R. 1998, On-line determination of stellar atmospheric parameters T_{eff}, log g, [Fe/H] from ELODIE echelle spectra. I. The method. A&A, 338, p151-160.

Kenworthy, M. A., Hinz, P. M., and Angel, J. R. P. 2000, Direct Detection of Thermal Emission from Extra-Solar Planets. in Planetary Systems in the Universe, IAU Symp. no. 202

Kürster, M., Endl, M., Els, S., Hatzes, A. P., Cochran, W. D., Döbereiner,

S., and Dennerl, K. 2000, An extrasolar giant planet in an Earth-like orbit. Precise radial velocities of the young star ι Horologii = HR 810. A&A, 353, L33-L36.

Lagage, P. -O. 2000, VISIR and the Detection of Exo-Planets. in From Extrasolar Planets to Cosmology: The VLT Opening Symp., eds. J. Bergeron & A. Renzini (Berlin : Springer-Verlag), 528

Lin, D. N. C., Bodenheimer, P., and Richardson, D. C. 1996, Orbital migration of the planetary companion of 51 Pegasi to its present location. Nature 380, 606-607.

Lissauer, J. J. 1999, Planetary Formation: From The Earth-Moon System To Extrasolar Planets. Bioastronomy 99: A New Era in Bioastronomy. 6th Bioastronomy Meeting-Kohala Coast Hawaii-Aug. 2-6.

Maddox, J. 1994, The Future History of the Solar System. Nature 372, 611.

Marcy, G. W., Butler, R. P., Williams, E., Bildsten, L., et al. 1997, The Planet around 51 Pegasi. ApJ, 481, 926.

Marcy, G. W., Vogt, S., Fischer, D., and Butler, R. P. 2000, Extrasolar Planets by Precise Velocities. AAS, 196.

Mayor, M., and Queloz, D. 1995, A Jupiter-Mass Companion to a Solar-Type Stars. Nature 378, 355.

McElroy, M. B. 1972, Mars ; an evolving atmosphere. Science 175, 443-445.

Neuhäuser, R., Brandner, W., Echark, A., et al. 2000, On the possibility of ground-based direct imaging detection of extra-solar planets: the case of TWA-7. A&A, 354, L9-L12.

Peale, S. J. 1977, Rotation histories of the natural satellites. in Planetary Satellites (ed. Burns, J. A.) (Univ. of Arizona Press, Tucson) pp. 87-112.

Peale, S. J., Cassen, P., and Reynolds, R. T. 1979, Melting of Io by tidal dissipation. Science 203, 892-894.

Perryman, M. A. C. 1997, Recent Results from HIPARCOS. American Astron. Soc. Meeting. 191.

Queloz, D., Mayor, M., Neaf, D., et al. 2000, Extrasolar Planets in the Southern Hemisphere: The CORALIE Survey. in From Extrasolar Planets to Cosmology: The VLT Opening Symposium, Proc. of the ESO Symp., eds. J. Bergeron & A. Renzini (Berlin : Springer-Verlag), p548

Queloz, D., Mayor, M., Weber, L., et al. 2000, The CORALIE survey for Southern extra-solar planets. I. A planet orbiting the star Gliese 86. A&A, 354, p99-102.

Rasio, F. A., and Ford, E. B. 1996, Dynamical instabilities and the formation of extrasolar planetary systems. Science 274, 954-956.

Rasio, F. A., Tout, C. A., Lubow, S. H., and Livio, M. 1996, Tidal decay of close planetary orbits. ApJ, 470, 1187.

Rauer, H., Harris, A., Collier Cameron, A., and Export Team. 2000, Search for signatures of atmospheres/exopheres in extra-solar planets. IAU

Reimers, D. 1975, Circumstellar envelopes and mass loss of red giant stars. (In : Problems in stellar atmospheres and envelopes.) p229-256.

Rhie, S. H., Bennett, D. P., Clampin, M., et al. 2000, The Galactic Exoplanet Survey Telescope (GEST) : A Search for Extra-Solar Planets via Gravitational Microlensing and Transits. American Astron. Soc. DPS meeting.

Rocha-Pinto, H. J., and Maciel, W. J. 1998, Consistency of the metallicity distributions of nearby F, G and K dwarfs. A&A, 339, 781-801.

Sackmann, I. -Juliana., Boothroyd., Arnold I., and Kraemer, K. E. 1993, Our Sun. III. Present and Future. ApJ, 418, 457.

Santos, N. C., Mayor, M., Naef, D et al. 2000a, The CORALIE survey for Southern extra-solar planets. IV. Intrinsic stellar limitations to planet

searches with radial-velocity techniques. A&A, 361, p265-272.

Santos, N. C., Mayor, M., Naef, D., et al. 2000b, The CORALIE survey for Southern extra-solar planets. III. A giant planet in orbit around HD 192263. A&A, 356, p599-602.

Schneider, J. 2000, Extrasolar Planets Ttansits : Detection and Follow-Up. in From Extrasolar Planets to Cosmology: The VLT Opening Symp. eds. J. Bergeron & A. Renzini (Berlin : Springer-Verlag), p499

Shklovski, I. S., and Sagan, C. 1966, Intelligent Life in the Universe. (Holden-Day, San Francisco).

Soubiran, C., Katz, D., and Cayrel, R. 1998, On-line determination of stellar atmospheric parameters T_{eff}, $\log g$, [Fe/H] from ELODIE echelle spectra. II. The library of F5 to K7 stars. A&AS, 133, p221-226.

Turcotte, D. L. 1996, Magellan and comparative planetology. J.Geophys. Res. 101, 4765-4773.

Udry, S., Mayor, M., Naef, D., et al. 2000, The CORALIE survey for Southern extra-solar planets. II. The short-period planetary companions to HD 75289 and HD 130322. A&A, 356, p590-598.

Vogt S. S., Marcy, G. W., Butler, R. P., and Apps, K. 2000, Six New Planets from the Keck Precision Velocity Survey. ApJ, 536, 902-914.

Walker, J. C. G. 1977, Evolution of the Atmosphere. Macmillan, New York.

Walker, J. C. G., Hays, P. B., and Kasting, J. F. 1981, A negative feedback mechanism for the long-term stabilization of Earth's surface temperature. J. Geophys. Res. 86, 9776-9782.

Walker, J. C. G. 1991, Feedback processes in the biogeochemical cycles of carbon. In Scientists on Gaia (S. H. Schneider and P. J. Boston, Eds.), pp. 183-190. MIT press. Cambridge, MA.

Wetherill, G. W. 1996, The formation and habitability of extra-solar planets.

Icarus 119, 219-238.

Whitmire, D. P., Matese, J. J., and Tomley, L. J. 1988, A brown dwarf companion as an exoplanation of the asymmetry in the Beta Pictoris disk. A&A, 203, L13-L15.

Williams, D. M., Kasting, J. F., and Wade, R. A. 1997, Habitable Moons around Extrasolar Giant Planets. Nature 385, 234-236.

Williams, D. M. 1998, The Stability of Habitable Planetary Environments. Submitted thesis in Degree of Dr. of Philosophy. Univ. Pennsylvania.

Wolszczan, A., Cordes, J. M., and Dewey, R. J. 1991, Discovery of a young, 267 millisecond pulsar in the supernova remnant W44. ApJ, 372, L99-L102.